Systems/Circuits

Activity of Spinal Interneurons during Forward and Backward Locomotion

Pavel E. Musienko,[1,2,3] Vladimir F. Lyalka,[4] Oleg V. Gorskii,[1,2] Pavel V. Zelenin,[4] and Tatiana G. Deliagina[4]

[1]Laboratory of Neuroprosthetics, Institute of Translational Biomedicine, St. Petersburg State University, St. Petersburg 199034, Russia, [2]Laboratory of Motor and Visceral Functions Neuromodulation, Pavlov Institute of Physiology, St. Petersburg 199034, Russia, [3]Sirius National Technical University, Sochi 354340, Russia, and [4]Department of Neuroscience, Karolinska Institute, SE-17177 Stockholm, Sweden

Higher vertebrates are capable not only of forward but also backward and sideways locomotion. Also, single steps in different directions are generated for postural corrections. While the networks responsible for the control of forward walking (FW) have been studied in considerable detail, the networks controlling steps in other directions are mostly unknown. Here, to characterize the operation of the spinal locomotor network during FW and backward walking (BW), we recorded the activity of individual spinal interneurons from L4 to L6 during both FW and BW evoked by epidural stimulation (ES) of the spinal cord at L5–L6 in decerebrate cats of either sex. Three groups of neurons were revealed. Group 1 (45%) had a similar phase of modulation during both FW and BW. Group 2 (27%) changed the phase of modulation in the locomotor cycle depending on the direction of locomotion. Group 3 neurons were modulated during FW only (Group 3a, 21%) or during BW only (Group 3b, 7%). We suggest that Group 1 neurons belong to the network generating the vertical component of steps (the limb elevation and lowering) because it should operate similarly during locomotion in any direction, while Groups 2 and 3 neurons belong to the networks controlling the direction of stepping. Results of this study provide new insights into the organization of the spinal locomotor circuits, advance our understanding of ES therapeutic effects, and can potentially be used for the development of novel strategies for recuperation of impaired balance control, which requires the generation of corrective steps in different directions.

Key words: **decerebrate cat; epidural stimulation; locomotion; sensory feedback; spinal neurons**

Significance Statement

Animals and humans can perform locomotion in different directions in relation to the body axis (forward, backward, sideways). While the networks that control forward walking have been studied in considerable detail, the networks controlling steps in other directions are unknown. Here, by recording the activity of the same spinal neurons during forward and backward walking, we revealed three groups of neurons forming, respectively, the network operating similarly during stepping in different directions, the network changing its operation with a change in the direction of stepping, and the network operating only during locomotion in a specific direction. These networks presumably control different aspects of the step. The obtained results provide new insights into the organization of the spinal locomotor networks.

Introduction

All vertebrates can control the direction of locomotor movements relative to the front-to-rear body axis. Thus, in addition to forward locomotion, which is the main form of locomotion for most living beings, legged vertebrates can walk in any direction in relation to the body axis (backward, sideways), as well as to perform stepping in place (Stein et al., 1986; Thorstensson, 1986; Buford et al., 1990; Buford and Smith, 1990; Eilam and Shefer, 1992; Rossignol, 1996; Ashley-Ross and Lauder, 1997; Vilensky and Cook, 2000; Vemula et al., 2019). Backward and sideways locomotion are usually generated in the context of avoidance behavior. In addition, single steps in different directions are generated for postural corrections to restore balance or the basic body configuration perturbed during standing (Beloozerova

Received Sep. 16, 2021; revised Feb. 21, 2022; accepted Mar. 13, 2022.

Author contributions: P.E.M., V.F.L., P.V.Z., and T.G.D. designed research; P.E.M., V.F.L., O.V.G., P.V.Z., and T.G.D. performed research; P.E.M., V.F.L., O.V.G., P.V.Z., and T.G.D. analyzed data; P.E.M. and T.G.D. wrote the paper.

This work was supported by the St. Petersburg State University, St. Petersburg, Russia (project ID: 73025408) to P.E.M. and O.V.G.; by National Institutes of Health Grant R01-NS-100928 to T.G.D. and P.E.M.; by Swedish Research Council Grants 2017-02944 and 2020-02502 to T.G.D.; and by Russian Foundation for Basic Research Grant 20-015-00568 and Russian Science Foundation Grant 21-15-00235 to P.E.M. We thank Polina Shkorbatova and Natalia Merkulyeva for help with the histological evaluation.

The authors declare no competing financial interests.

Correspondence should be addressed to Tatiana G. Deliagina at Tatiana.Deliagina@ki.se.

https://doi.org/10.1523/JNEUROSCI.1884-21.2022

et al., 2003; Karayannidou et al., 2009; Hsu et al., 2017) and FW locomotion (Musienko et al., 2014).

While the neural mechanisms responsible for the control of forward locomotion have been studied in considerable detail (for review, see Grillner, 1975; Grillner and Zangger, 1979; Orlovsky et al., 1999; Rossignol et al., 2006; Kiehn, 2016), our knowledge about the neural mechanisms generating locomotion in other directions is scarce (Deliagina et al., 2019). Although the comparison of the kinematics of forward walking (FW) and backward walking (BW) in humans and animals has revealed substantial differences (Thorstensson, 1986; Buford et al., 1990; Eilam and Shefer, 1992; Ashley-Ross and Lauder, 1997; Vemula et al., 2019), the analysis of the muscle activity patterns revealed similar basic flexor–extensor synergies (Pratt et al., 1996; Jansen et al., 2012; Zelik et al., 2014; Harnie et al., 2021). It has been suggested that there are some common direction-independent neuronal networks contributing to the generation of both FW and BW.

It has been shown that BW can be evoked by electrical epidural stimulation (ES) of the spinal cord in decerebrate and spinal-transected (spinal) subjects (Musienko et al., 2007; Courtine et al., 2009; Shah et al., 2012), as well as by perineal stimulation in spinal cats (Harnie et al., 2021). Thus, not only basic FW but also BW movements are generated by spinal networks. Experiments on a split-belt treadmill demonstrated that, as during FW (Forssberg et al., 1980; Frigon et al., 2017), the stepping of each limb during BW is generated by a separate network (Harnie et al., 2021; Lyakhovetskii et al., 2021).

Previously, we demonstrated that ES of certain sites of the spinal cord can evoke stepping in any direction relative to the body axis and the direction of locomotion is determined by the direction of treadmill belt motion, while on an unmovable surface, in-place stepping is observed (Musienko et al., 2012). We suggested that the locomotor system includes two principal mechanisms, one generating a vertical component of the step (limb elevation and lowering), and the other generating a horizontal component (limb transfer from one extreme point to the other along the direction of locomotion). The latter includes networks generating the horizontal component of the step in different directions. It was also suggested that the same mechanisms generate a single corrective step in a particular direction in response to sensory information signaling a distortion of balance or body configuration (Hsu et al., 2017).

The vertical component of the step is generated during stepping in any direction, while the horizontal component is specific to each direction. We hypothesize that individual neurons forming the network generating the vertical component of the step have the same phase of activity in the locomotor cycle during walking in any direction, while the activity of neurons that are elements of the networks generating the horizontal component of the step is strongly modified with a change of stepping direction. The activity of individual spinal neurons during locomotion in different directions has not been studied. Here, we test our hypothesis by recording the activity of the same individual spinal neurons during both FW and BW evoked by ES in decerebrate cats. The obtained results support our hypothesis.

Materials and Methods

Experiments were conducted on four adult cats of either sex (weight range, 2.5–4.0 kg). All procedures were conducted in accordance with protocols (#01a/2017 and #01a/2018) approved by the Animal Care Committee of the Pavlov Institute of Physiology (St. Petersburg, Russia), and adhered to the European Community Council Directive (2010/63EU) and the guidelines of the National Institutes of Health (*Guide for the Care and Use of Laboratory Animals*).

Surgical procedures. The surgical procedures were similar to those in our previous studies (Merkulyeva et al., 2018; Musienko et al., 2020). The cats were deeply anesthetized with isoflurane (2–4%) delivered in O_2. For the induction of anesthesia, xylazine (0.5 mg/kg, i.m.) was injected. The level of anesthesia was monitored based on applying pressure to a paw (to detect limb withdrawal), as well as by checking the size and reactivity of the pupils. The trachea was cannulated, and the carotid arteries were ligated. The animals were decerebrated at the precollicular-postmammillary level. A laminectomy was performed between the L4 and L7 segments for ES and recording of neurons. The exposed dorsal surface of the spinal cord was covered with warm paraffin oil. Bipolar electromyographic (EMG) electrodes (0.2 mm flexible stainless steel Teflon-insulated wires; catalog #AS632, Cooner Wire) were implanted bilaterally into the m. gastrocnemius lateralis (Gast; ankle extensor, and knee flexor) and m. tibialis anterior (Tib; ankle flexor), as described previously (Gerasimenko et al., 2009). Anesthesia was discontinued after the surgical procedures. The experiments were started 2–3 h thereafter.

During the experiment, the rectal temperature and mean blood pressure of the animals were continuously monitored. The rectal temperature was maintained at 37 ± 0.5°C with the help of heat irradiation. The blood pressure was kept at >80 mmHg. If needed, the injection of prednisolone (3 mg/kg, i.m.) was performed to stabilize the arterial pressure and to reduce brain swelling after decerebration.

Experimental design. The experimental design (Fig. 1*A*) was similar to that used in our previous study (Musienko et al., 2020). The head, the vertebral column, and the pelvis of the decerebrate cat were fixed in a rigid frame. The forelimbs had no support, whereas the hindlimbs were positioned on the treadmill with two separate belts (left and right) moving at the same speed (0.5 m/s) and below referred to as the "treadmill belt." The distance between the treadmill belt and the fixed pelvis was 21–25 cm (depending on the animal size), which determined a hemiflexed limb configuration in the middle of stance typical for walking. The treadmill belt was moving either backward or forward in relation to the animal.

In each cat, locomotion was evoked by ES of the spinal cord (Iwahara et al., 1992; Musienko et al., 2007, 2012; Gerasimenko et al., 2009; Merkulyeva et al., 2018). The stimulation started 2–3 s after onset of the treadmill belt motion. For ES, a ball electrode ($d = 0.5$ mm) was positioned on the dura mater in the middle of the dorsal surface of the spinal cord at the L5–L6 level (Fig. 1*A*, ES). A syringe needle in the dorsal muscles was used as a reference electrode for ES. The site of ES stimulation that produced well coordinated FW and BW on the treadmill belt moving backward and forward, respectively, was used (Merkulyeva et al., 2018). We used the following parameters of stimulation: bipolar square pulses, frequency, 5 Hz; pulse duration, 0.2–0.5 ms; current, 100–300 μA.

The left and right side views of the walking cat were recorded by two video cameras (50 frames/s; model HDR-CX160E, Sony). In addition, we recorded the anterior–posterior locomotor limb movements by means of two custom-made mechanical sensors, one of which, Limb-L, is shown in Figure 1*A*. The sensor consisted of a high-resolution variable resistor, the axis of which was rotated by means of a long lever attached to the limb.

Recording of neurons. In the present study, spinal neurons were recorded extracellularly from the spinal segment L4–L6 by means of commercially available multichannel electrode arrays (ME; Fig. 1*A*). Each array consisted of a shaft with 32 Pt/Ir/Au electrode sites (A1x32-10 mm-50–177; NeuroNexus). Each site surface area was 177 μm^2 with impedance of ~1 MΩ at 1 kHz. Electrode sites were distributed 50 μm apart vertically. Thus, the recording length of the array was ~1.5 mm, which allowed for simultaneous recordings of many individual neurons from different areas of the gray matter. The array was mounted on an electrode holder driven by a manual micromanipulator. To increase the stability of the recording that is to prevent displacement of the nervous tissue in relation to the recording electrodes caused by movements (e.g., locomotor, breathing), the exposed dorsal surface of the spinal cord was covered with warm paraffin oil, the space between the dura mater and

the walls of the spinal canal was filled with tissue adhesive glue (Indermil X Fine, Henkel Ireland Operations and Research Limited) in the area of recording.

We attempted to explore systematically the whole cross section of the gray matter except for the areas of motor nuclei. However, histologic verification of the array track positions showed that while in L4 and L6 segments the array track positions covered the whole cross section of the gray matter, in the L5 spinal segment all array tracks were positioned in the medial part of the gray matter. Recording of putative spinal interneurons at the same position of the array in the gray matter was performed during the 7–10 s before the treadmill was switched on (to reveal the spontaneous activity of neurons), during FW evoked by ES on a backward-moving treadmill belt, during BW caused by a reverse in the direction of the treadmill belt motion, and, finally, again during FW. In most cases, this same recording procedure was repeated twice with 5–15 min of rest (no ES stimulation). Such a procedure allowed distinguishing between neurons, which are active during locomotion in one direction only, from neurons in which activity disappeared/appeared because of displacement of the array in relation to the tissue. The latter were not included in the analysis. Under each condition, the neuronal activity was recorded in ~20–60 locomotor cycles.

In addition, to estimate the possible contribution of sensory feedback from the limb to the locomotor modulation of a neuron, the majority of neurons was recorded during passive movements of the ipsilateral and passive movements of the contralateral limb performed manually along the FW and BW trajectory. For this purpose, in the resting animal with no ES, one of the hindlimbs was suspended while the other one (held by the metatarsus) was moved forward from the posterior extreme position (similar to that observed at the end of the stance during FW) to the anterior extreme position (similar to that observed at the end of swing during FW) where the limb was landed (imitation of swing). Then the limb was moved backward together with the moving treadmill belt (imitation of stance). To move the limb along the BW trajectory, the limb was moved backward from the anterior extreme position (similar to that observed at the end of stance during BW) to the posterior extreme position (similar to that observed at the end of swing during BW) where the limb was landed (imitation of swing). Then the limb was moved forward together with the moving treadmill belt (imitation of stance). At each position of the electrode array, neurons were recorded during 5–10 cycles of passive movements along the FW trajectory and during 5–10 cycles of passive movements along the BW trajectory performed by each of the hindlimbs.

To determine the approximate location of individual neurons (recorded at a definite position of the array by a particular electrode site) on the spinal cord cross section, the lateral and vertical coordinates of the array tip were marked.

The signals from the electrode array (neuronal activity), EMG electrodes, and mechanical sensors were amplified and digitized with a sampling frequency of 24 kHz (neurons), 20 kHz (EMGs), and 5 kHz (sensors). Neuronal activity was bandpass filtered in the ranges 2.2–7500 Hz (Medusa preamplifiers, Tucker-Davis Technologies) and 300–6000 Hz (digital), and EMGs were filtered only on the amplifier stage in the range 100–5000 Hz (model 1700 Differential AC Amplifier, A-M Systems). These signals, together with the signals indicating the switching-on and switching-off of the treadmill and ES, were recorded on a computer disk using a data acquisition system (RZ5 BioAmp Processor, Tucker-Davis Technologies). For synchronization of the video recording with other recorded signals, synchro pulses were used that were recorded by the acquisition system, and produced light flashes recorded by video cameras.

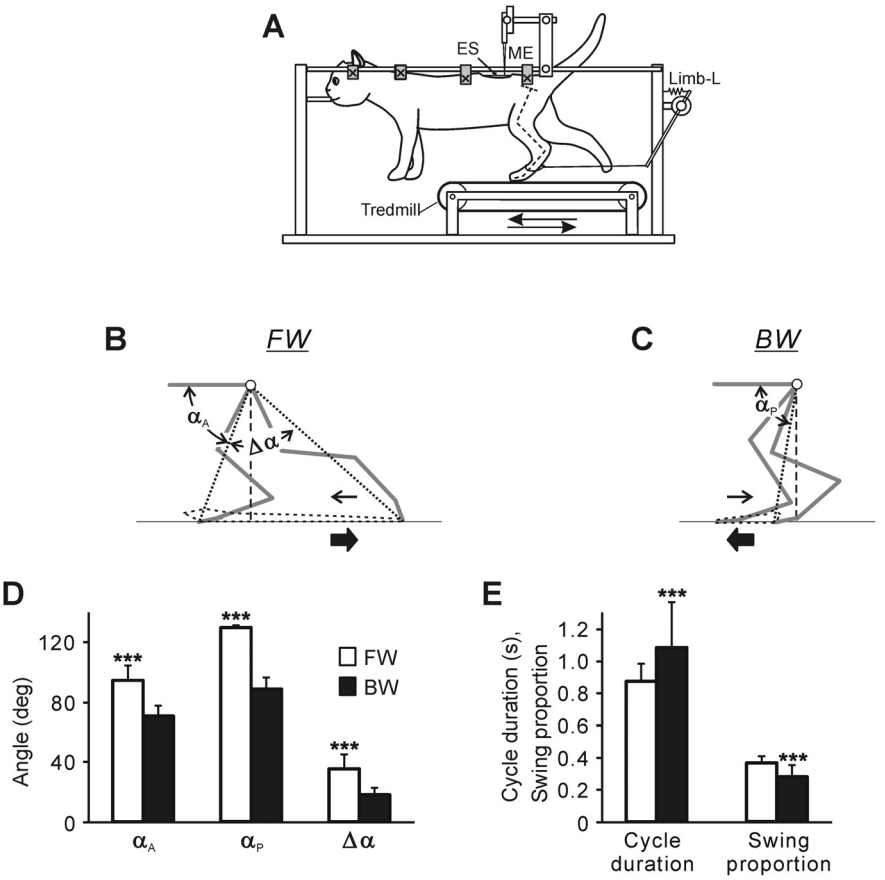

Figure 1. Experimental design and comparison of FW and BW movements evoked by ES of the L5. ***A***, The head, vertebral column, and pelvis of a decerebrate cat were fixed in a rigid frame (points of fixation are indicated by X). The hindlimbs were positioned on the treadmill. Walking of the hindlimbs was evoked by the ES of the spinal cord. A change in the direction of locomotion from forward to backward was caused by a change in direction of the treadmill belt motion, respectively, from backward to forward relative to the animal (indicated by arrows). Anterior/posterior movements of each limb were recorded by mechanical sensors (only the left sensor, Limb-L, is shown). Neuronal activity was recorded by an ME. ***B***, ***C***, Extreme positions of the left hindlimb during one forward (***B***) and backward (***C***) step cycle. Angles α_A and α_P characterize the extreme anterior and posterior paw positions in relation to the trunk, respectively. Angle $\Delta\alpha$ characterizes the amplitude of limb movements. Thick and thin arrows indicate directions of the treadmill belt movement and the foot movement during swing, respectively. ***D***, ***E***, Comparison of characteristics of FW and BW evoked by ES (mean ± SD). In ***D*** and ***E***, $N = 3$, $n = 60$; and $N = 4$, $n = 60$, respectively. ***$p < 0.001$.

Data analysis. The multiunit spike trains recorded by each electrode were separated into unitary waveforms representing the activity of individual neurons using the spike-sorting procedure in analysis software (Spike2, Cambridge Electronic Design). The spikes with the same waveform were assumed to be generated by the same spinal neuron during FW and BW (Fig. 2*A*,*B*,*D*). Only neurons with a stable spike shape and a high signal-to-noise ratio were used for the analysis. Many neurons were recorded simultaneously by several neighboring sites, which increased the confidence of the spike sorting. An example of activity of nine neurons simultaneously recorded during FW and BW, their positions on the cross section of the gray matter, as well as waveforms of their spikes are shown in Figure 2*A–D*, respectively.

Since the main kinematic difference that discriminates FW from BW is the direction of the limb movement during stance and swing, we compared activity of individual neurons in these two main phases of the FW

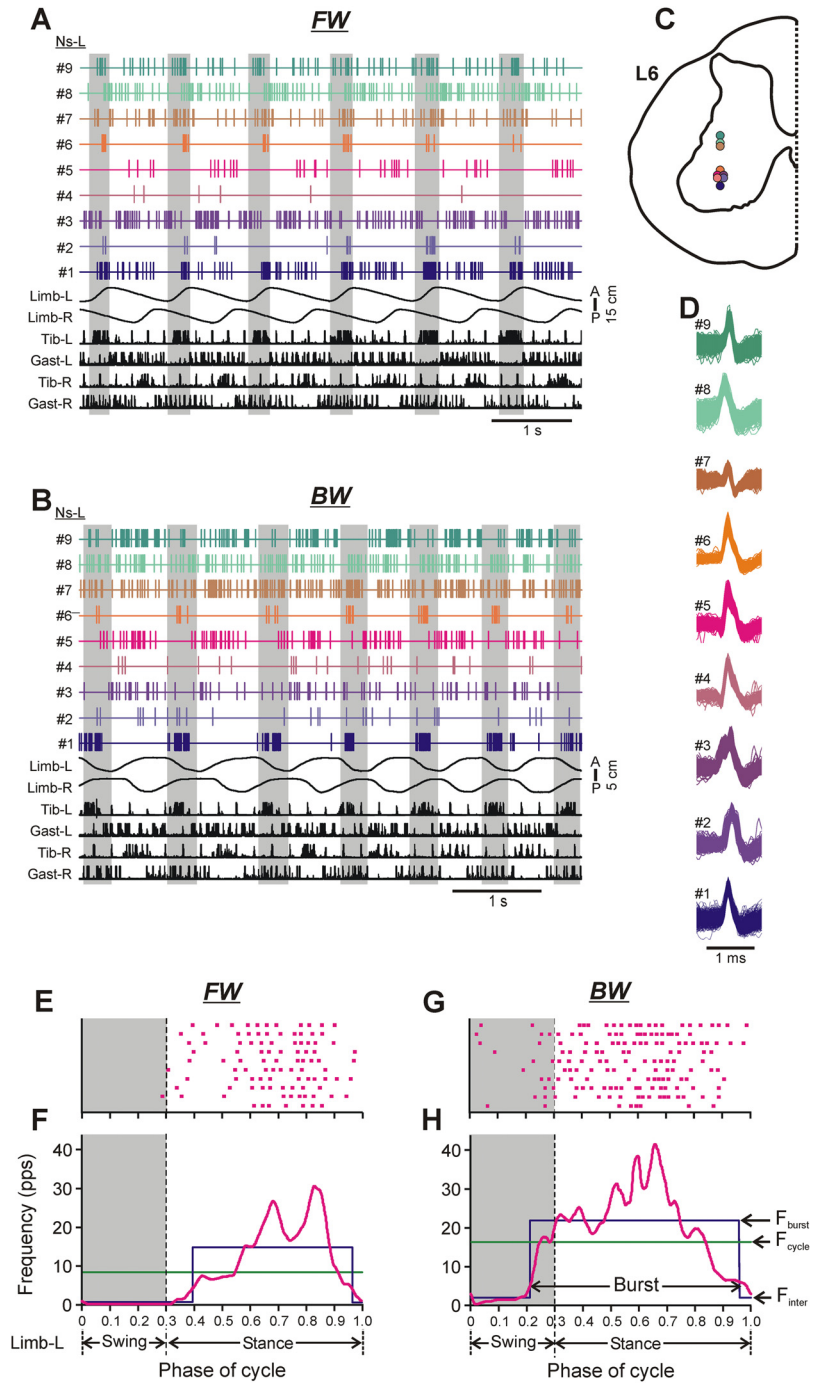

Figure 2. Activity of the same spinal neurons during FW and BW. ***A–D***, Location of nine spinal neurons (#1–9) recorded simultaneously by the multichannel electrode array on the left side of L6 (***C***), overdrawn waveforms of their spikes extracted from the mass activity by spike-sorting procedure (***D***), as well as their activity during FW and BW (***A*** and ***B***, respectively). Neuronal activity was recorded along with movements of the left and right limbs (Limb-L and Limb-R), and EMGs of the left (L) and right (R) gastrocnemius and tibialis muscles (Gast-L, Gast-R, and Tib-L, Tib-R, respectively). The EMGs were rectified. The EMG signals contained large responses to individual epidural stimuli. Swing phases of the left hindlimb are highlighted. ***E–H***, The rasters (***E***, ***G***; for clarity, only 10 of 20–60 recorded cycles are shown) and the histograms (***F***, ***H***) of the activity of neuron #5 in the cycle of the ipsilateral hindlimb during FW (***E***, ***F***) and BW (***G***, ***H***). The swing phase is highlighted. ***F***, ***H***, The violet lines show the best two-level rectangular approximations of the histograms, with the burst period (top level indicating also the mean burst frequency, F_{burst}) and interburst period (bottom level indicating also the mean interburst frequency, F_{inter}). The green lines show the mean cycle frequency (F_{cycle}).

and BW cycle. The activity of the neurons was typically modulated with the locomotor rhythm (Fig. 2*A*, *B*). To characterize this modulation, a phase histogram of neuronal activity in a step cycle was created. Because of some variability in the duration and structure of step cycles within tests with locomotion in a particular direction, as well as difference in the duration and structure of the step cycle in the tests with FW and BW (Merkulyeva et al., 2018), we used dual-referent phase analysis (Berkowitz and Stein, 1994); that is, we normalized the swing and stance phase separately. The swing was normalized to the swing proportion in the locomotor cycle averaged across all episodes of FW and BW in all cats. The stance was normalized correspondingly. Normalized swing and stance constituted 30% and 70% of the locomotor cycle, respectively. Such normalization ensured that neuronal activity during a definite phase (swing or stance) of FW was compared with the activity during the same phase of BW or when these characteristics were compared in different steps within the same test.

The spike time sequence of an individual neuron was converted to the instantaneous rate versus time and then to the instantaneous rate versus phase (300 points for the swing, 700 points for the stance). The dependence of the instantaneous rate on the phase was averaged over all steps of a given test. Then the histogram was smoothed (sliding averaging, window width, 30 bins) to remove high-frequency noise. Examples of the rasters and the resulting histograms are shown in Figure 2*E–H*.

To evaluate the depth of step-related modulation of neuronal activity, we used the best two-level rectangular fit for the entire activity histogram (Zelenin et al., 2011); the upper and lower levels were defined as a mean burst and interburst frequency, respectively (Fig. 2*H*; Zelenin et al., 2011). Also, for each neuron, the mean cycle frequency (Fig. 2*H*) was calculated for the entire activity histogram, and the mean frequency of spontaneous activity (recorded before the treadmill was switched on) was calculated.

The activity of neurons was considered modulated if, first, the mean burst frequency was significantly different from the mean interburst frequency (Student's t test, $p < 0.05$) and, second, the pattern of modulation in the majority of the locomotor cycles was consistent (the Pearson's correlation coefficient between the profiles of the activity in individual locomotor cycles and in the entire activity histogram was >0.3 in >60% of the locomotor cycles). These criteria were always stricter than with Rayleigh's test ($p < 0.01$). The coefficient of frequency modulation was defined as $K_{mod} = (1 - F_{inter}/F_{burst}) \times 100\%$, where F_{inter} and F_{burst} are mean interburst and burst frequencies, respectively.

To reveal the mean and the variability of the activity phase of an individual neuron in the locomotor cycle, the instantaneous frequency of the neuron versus the normalized phase of the locomotor cycle (see above) was used. The best two-level rectangular fit for instantaneous frequency of the neuron within each individual step cycle was used to determine its burst onset and burst offset phases in this cycle. Then the mean ± SD for the burst onset phase and for the burst offset phase were calculated across all step cycles using circular statistics methods (Batschelet, 1981).

To reveal groups of neurons with similar activity phases during FW as well as during BW, we used a modified version of the k-means method of cluster analysis similar to the method used by Krouchev et al.

(2006). For each neuron, its activity phases were presented in the 4D space with the following coordinates: (1) the mean ± SD burst onset phase during FW; (2) the mean ± SD burst offset phase during FW; (3) the mean ± SD burst onset phase during BW; and (4) the mean ± SD burst offset phase during BW.

We did not specify the number of clusters a priori. The clustering procedure consisted of the following three stages: (1) ranking neurons according to the stability of their activity; (2) primary clustering ("seeding") that produced an initial set of "raw" clusters; and (3) "refining" of the" raw" clusters.

First, we ranked all neurons according to the stability of their activity phase, reflected in SDs of the onset and offset phases, since we supposed that neurons with stable phase of activity have larger contribution to control of locomotor movements. For this purpose, we converted SDs into "weights" by using the following formula, which is similar to a sigmoid function: $w = 10/(1 + 900\mathrm{SD}^2)$. Thus, neurons with higher variability (i.e., neurons with unstable activity, and therefore a larger SD) had lower weight of their phase, and vice versa. Then the integral stability of the activity phase of the neuron during FW and BW (W) was calculated as follows: $W = (w_{\mathrm{onFW}})^2 + (w_{\mathrm{offFW}})^2 + (w_{\mathrm{onBW}})^2 + (w_{\mathrm{offBW}})^2$, where w_{onFW}, w_{offFW}, w_{onBW}, and w_{offBW} were the weights of the onset and offset phases during FW and BW, respectively. Then, all neurons in the list were ranked according to their W.

For primary clustering, the point in the 4D space corresponding to the first neuron in the ranked list (characterizing the onset and offset of the neuron during FW and BW) was considered as the first cluster. Then points of other neurons were compared one by one with already existing clusters. Closeness or remoteness of a point from the centers of the existing clusters was characterized by the following two parameters: Euclidian distance (D) and Z-distance (Z). If at least one of these distances exceeded the threshold level ($D > 0.3$ or $Z > 5$) the point gave rise to a new cluster. If the point was close to one or several clusters ($D < 0.3$ and $Z < 5$), it was merged with the cluster for which D was minimal. For this expanded cluster, its center was recalculated. The center of the cluster (i.e., the average onset and offset phases during FW and BW for neurons composing the cluster) was calculated by using the weighted average for a phase of onset (Φ^{on}) or offset (Φ^{off}): $\Phi = \Sigma(w\varphi)/\Sigma w$, while the weighted average SD was calculated by the following formula: $\mathrm{SD} = \Sigma(w\mathrm{SD})/\Sigma w$.

The set of clusters obtained during the primary (seeding) clustering was used to resort the points with a refining procedure, similar to seeding but by using stricter criteria, as follows: the point was considered far from the center of the cluster if $D > 0.15$ or $Z > 4$. In such a case, it was considered to be "assorted" (added to cluster 0). If the point was close to one or several clusters ($D < 0.15$ and $Z < 4$), it was merged with the cluster for which D was minimal. This resorting was repeatedly applied to the entire ranked list of neurons until convergence to the final set of clusters.

In addition, for each cluster the midburst phase Φ^{mid} during a particular direction of locomotion (FW or BW) was calculated as $\Phi^{\mathrm{mid}} = (\Phi^{\mathrm{on}} + \Phi^{\mathrm{off}})/2$. For an individual cluster, the difference between the midburst phases observed during FW and BW was used to categorize this cluster as a cluster with similar or different phases of activity during FW and BW.

To reveal the possible contribution of movement-related sensory inputs from the ipsilateral and the contralateral hindlimb to the modulation of individual neurons during FW and BW, a part of the neurons was recorded during both passive movements of the ipsilateral hindlimb and during passive movements of the contralateral hindlimb performed along both the FW and BW trajectories. For neurons that were modulated by passive movements of the limbs, we tried to assess a possible contribution of this sensory-produced modulation to their modulation during FW and BW. For this purpose, for each neuron that was modulated by passive movements performed by either hindlimb, first, we compared the phase of its modulation in the cycle of the ipsilateral limb movement with that observed in the cycle of the contralateral limb movement. If the neuron had the same phase of modulation in the cycle of the ipsilateral and in the cycle of the contralateral limb movement along FW as well as BW trajectories, the sensory inputs from the limbs cannot explain the locomotor modulation of these neurons since during both FW and BW the hindlimbs moved in antiphase. If the neuron had either opposite phases of modulation in the cycles of ipsilateral and contralateral limb movement (e.g., in the middle of the stance during ipsilateral limb movement and in the swing during contralateral limb movement, or at the end of the stance during ipsilateral limb movement and at the beginning of stance during contralateral limb movement), such a neuron received complementary sensory inputs from the two limbs, which could potentially contribute to locomotor modulation of these neurons. Second, to find out whether it was the case, we compared the phase of the modulation of these neurons in the cycle of the ipsilateral limb during locomotion in a particular direction with that observed during passive movements of the ipsilateral limb along the locomotor trajectory in the same direction. If the neuron with complementary sensory inputs had the phase of modulation similar under the two conditions, it was suggested that modulation of this neuron during locomotion can be explained by sensory feedback from the hindlimbs. If the phases of modulation largely overlapped under the two conditions (the phase of the burst in one of the conditions was within the phase of the burst observed in another condition; Musienko et al., 2020), it was suggested that sensory feedback from the hindlimbs can potentially contribute to modulation of these neurons during locomotion. Finally, if the phases of modulation under the two conditions were different, it was suggested that locomotor modulation of this neuron cannot be explained by sensory feedback from the limb. For neurons that were modulated by passive movements of one hindlimb only, the similar procedure was used to reveal the possible contribution of sensory feedback to locomotor modulation. However, the phase of modulation during passive movements of the limb was compared with the phase of modulation in the cycle of the same limb during locomotion.

To characterize quantitatively the difference in the limb movement in relation to the trunk during FW and BW, we connected the hip with the tip of the paw at the extreme anterior and posterior limb positions in stance by lines and calculated angles between the pelvis and these lines (Fig. 1*B*,*C*, angles α_A, α_P, respectively). To evaluate the magnitude of limb oscillations, the angle between the extreme anterior and posterior limb positions (Fig. 1*B*, angle $\Delta\alpha = \alpha_P - \alpha_A$) was calculated. In each cat, the steps recorded in sequential FW and BW episodes were used. Then, we averaged a particular parameter across steps obtained in all cats during FW and BW.

Statistical analyses. All quantitative data in this study are presented as the mean ± SD. Paired Student's t test (two tailed) was used for pairwise comparisons. Welch's t test (two tailed) was used to characterize the statistical significance when comparing different means. To evaluate the statistical significance of difference in percentages of different types of modulated neurons recorded in L4, L5, and in L6, we used Pearson's χ^2 test. To compare a sample with a reference probability distribution or to compare two samples, we used a one-sample or two-sample Kolmogorov–Smirnov test, respectively. The significance level for all tests was set at $p = 0.05$.

Histologic procedures. At the termination of the experiments, the cats were deeply anesthetized with isoflurane (5%) and then perfused transcardially with isotonic saline followed by 4% paraformaldehyde solution, which caused death. The L4 and L6 spinal segments were removed from the spine and stored in 20% and 30% sucrose until they sank. Then, regions of segments containing the recording sites were cut on a freezing microtome into 50 μm frontal sections. The sections were collected in 0.1 M PBS, pH 7.4, and then stained with cresyl violet. The positions of the array in the spinal cord were verified by observation of the array tracks. The positions of the recording sites were estimated in relation to the array track position.

Results

Forward and backward locomotor movements evoked by ES

Examples of the FW and BW evoked by ES in the same cat are shown in Figure 2, *A* and *B*, respectively. In both cases, the right and left hindlimbs were stepping in antiphase. The EMG patterns were also similar in these two cases: the ankle extensor

Table 1. Neurons recorded in individual cats

	Active			
	Modulated	Nonmodulated	Inactive	Total (*n*)
Cat #1 (*L4*)	54	6	3	63
Cat #2 (*L5*)	107	17	8	132
Cat #3 (*L6*)	24	0	2	26
Cat #4 (*L6*)	158	46	11	215
Total (*n*)	343	69	24	436
Total (%)	79	16	5	100

Modulated, Neurons modulated during FW and/or BW; Nonmodulated, neurons that were active but nonmodulated during both FW and BW; Inactive, neurons that had a mean cycle frequency <1 Hz. The spinal segment in which neurons were recorded in a particular cat is indicated in parentheses by italic.

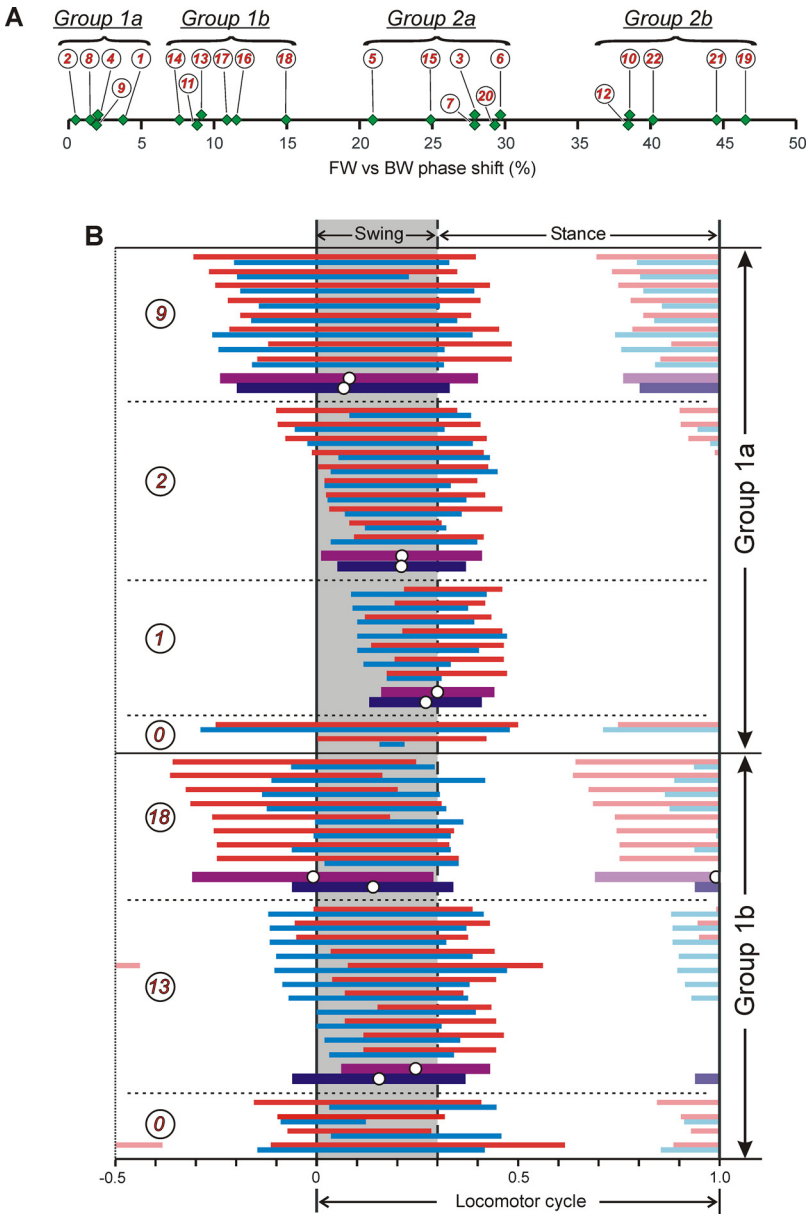

Figure 3. Phase characteristics of neurons. ***A***, The phase shift between the middle points of average bursts of individual clusters in the normalized FW and BW cycles. According to the value of the phase shift, all clusters can be combined into the following four populations: Group 1a, Group 1b, Group 2a and Group 2b. ***B***, Phase distribution of bursts of individual Group 1 swing neurons in normalized FW/BW locomotor cycle. Bursts of individual neurons during FW and BW are indicated by adjacent red and blue lines, respectively. Activity of the same neurons in neighboring cycles is indicated by the corresponding pale colors. The mean bursts of individual clusters during FW and BW with the middle point indicated (circles) are shown by thick purple and violet lines. Neurons of different clusters are demarcated by dotted lines. Numbers in circles are cluster numbers.

(Gast) was active during the stance phase of the limb, and the flexor (Tib) was active during the swing phase. The EMG signals during ES-evoked locomotion contained large short-latency responses to stimulating pulses coming at a frequency of 5 Hz (Fig. 2*A*,*B*). These general features of the two locomotor patterns were similar in all studied cats; they were also similar to those described in previous studies (Iwahara et al., 1992; Musienko et al., 2012; Merkulyeva et al., 2018).

However, the structure of the locomotor cycle, as well as the kinematics of locomotor movements during FW and BW, were different. As shown in Figure 1*E*, during BW the cycle duration was longer [mean ± SD, 1.09 ± 0.28 s ($N = 4$, $n_{ep} = 60$) vs 0.88 ± 0.11 s ($N = 4$, $n_{ep} = 60$), Welch's t test, $t_{(77)} = -5.35$, $p = 8.6 \times 10^{-7}$] compared with FW, and the swing proportion was a smaller [mean ± SD, 0.28 ± 0.07 ($N = 4$, $n_{ep} = 60$) vs 0.37 ± 0.04 ($N = 4$, $n_{ep} = 60$) fraction of cycle; Welch's t test, $t_{(98)} = 8.33$, $p = 5.1 \times 10^{-13}$].

The limb performed stepping at a more rostral position in relation to the trunk during BW than during FW (the values of angles α_A and α_P were 71 ± 6° and 94 ± 10° vs 89 ± 7° and 129 ± 2°, respectively; Welch's t test, $t_{(118)} = 14.81$ and $t_{(118)} = 41.37$, $p = 1.1 \times 10^{-28}$ and $p = 4.3 \times 10^{-72}$, respectively; Fig. 1*D*). Correspondingly, the magnitude of limb oscillations during BW locomotion was significantly smaller than that during FW (the value of $\Delta\alpha$ angle was 18 ± 5° vs 35 ± 9°; t test, $t_{(118)} = 12.58$, $p = 1.6 \times 10^{-23}$; Fig. 1*D*).

These results are similar to those described previously (Musienko et al., 2012, 2020; Merkulyeva et al., 2018). However, it should be noted that the kinematics of FW and BW caused by ES differ, to some extent, from those observed in intact cats (Buford et al., 1990; Buford and Smith, 1990). It was demonstrated that the kinematics of the hindlimb FW movements depended on the rostrocaudal position of the epidural electrode and that ES of the rostral and caudal segments of the lumbosacral enlargement causes FW, with predominance in the activity of flexors and extensors, respectively (Merkulyeva et al., 2018). Since in the rostral and caudal segments of the lumbosacral enlargement, motoneuronal pools of flexor and extensor muscles prevail, respectively (Vanderhorst and Holstege, 1997), it has been suggested that ES of a specific segment not only activates locomotor networks generating FW but also increases the level of excitability of motoneurons located in the stimulated and neighboring segments. In addition, the differences in the kinematics of BW could be caused by differences in the body configuration in which BW was performed. In our study, BW was performed with the spine fixed in a straight configuration that allowed us to record neuronal activity, while an intact cat performs BW with

flexion of the lumbar spine (Buford et al., 1990).

Characterization of neuronal database

Altogether, the activity of 436 individual spinal neurons was extracted from the multiunit spike trains recorded by the electrode array in the four cats, including 63, 132, and 241 neurons recorded in the L4, L5, and L6 spinal segments, respectively (Table 1). Of all the recorded neurons, rather few (5%) were "inactive" (i.e., they had a mean cycle frequency of <1 Hz, and thus, their contribution to the control of locomotion was very weak) or active but nonmodulated (16%; see criteria for modulation in Materials and Methods) during both FW and BW (Table 1). The majority of neurons (~86% from L4, ~81% from L5, and ~76% from L6) were active and modulated during FW and/or BW. Only these neurons were used for further analysis.

Classification of modulated neurons

Two hundred forty-five of 343 modulated neurons (~71%) exhibited modulation during both FW and BW. Each of the four phase parameters (FW onset, FW offset, BW onset, and BW offset phases) was distributed along the entire locomotor cycle. Continuous shifts in the active set of spinal interneurons during changes in locomotor speed were demonstrated in the larval zebrafish (McLean et al., 2007, 2008). Similarly, one could hypothesize that there was no discrete activation of different neuronal groups or populations in our dataset and that, instead, it represented a uniform, random distribution of activities. This hypothesis was rejected with the one-sample Kolmogorov–Smirnov test that compared a distribution of each of the four parameters (FW onset, FW offset, BW onset, and BW offset phases) with a uniform distribution (the corresponding significance levels were $p = 8 \times 10^{-25}$, 6×10^{-23}, 6×10^{-24}, and 6×10^{-21}, respectively).

To reveal subgroups of neurons with similar burst positions in the locomotor cycle during FW, as well as similar burst positions in the locomotor cycle during BW, these neurons were subjected to clustering (see Materials and Methods). One hundred seventy-nine neurons fell into 22 clusters. In 66 neurons, combinations of activity phases during FW and BW were unique, and we termed these "cluster #0".

To ensure that our "cluster" representation did not significantly distort the experimental data, we used the two-sample Kolmogorov–Smirnov test. For each of the four phase parameters (FW onset, FW offset, BW onset, and BW offset phases), we compared the experimentally obtained distribution with a distribution in which the phase of each neuron was replaced by the mean phase of a cluster to which the neuron belonged. We found that the difference was not statistically significant ($p = 0.33$, 0.08, 0.47, and 0.13, respectively). Moreover, if each of the four phase parameters (FW onset, FW offset, BW onset, and BW offset phases) for a neuron was replaced not by the mean phase of its cluster but by a random value from a Gaussian distribution with the mean and SD of its cluster, then the corresponding significance levels were $p = 0.98$, 0.99, 0.99, and 0.94, respectively. Therefore, we concluded that the presentation of the experimental data as a sample from a set of 22 clusters was adequate.

To reveal clusters with similar and different phases of activity during FW and BW, for each cluster, the difference between the midburst phases (the phase shift) during FW and BW was calculated. We applied hierarchical cluster analysis to the values of the phase shifts using the Ward (1963) variance minimization method. The elbow method (Thorndike, 1953) suggested the presence of two main groups (Figure 3*A*, Group 1 and Group 2).

Table 2. Different types of modulated neurons recorded in individual cats

	Cat #1 (L4)	Cat #2 (L5)	Cat #3 (L6)	Cat #4 (L6)	Total
Group 1	16 (30%)	53 (51%)	6 (30%)	70 (47%)	145 (45%)
Group 1a	6	21	2	34	63
Group 1b	10	32	4	36	82
Group 2	16 (30%)	17 (17%)	7 (35%)	42 (28%)	82 (25%)
Group 2a	12	12	3	23	50
Group 2b	4	5	4	19	32
Group 3	21 (40%)	33 (32%)	7 (35%)	37 (25%)	98 (30%)
Group 3a	12	30	7	26	75
Group 3b	9	3	0	11	23
Total	53	103	20	149	325 (100%)

Number of neurons in groups and subgroups recorded in individual animals is indicated. Percentage of neurons constituting individual groups in individual animals as well as in all animals is indicated in parentheses. Eighteen modulated neurons did not belong to any group and were not included in the analysis.

Each of these two groups consisted of two smaller groups (Figure 3*A*, Group 1a, Group 1b, Group 2a, and Group 2b).

Group 1 contained clusters with small phase shifts (up to 15% of the cycle), while Group 2 contained clusters with substantial phase shifts (between 21% and 47% of the cycle). Group 1a contained clusters (#1, #2, #4, #8, and #9) with almost the same midburst position in the FW and BW locomotor cycles (the phase shift from 0% to 4% of the cycle), and Group 1b contained clusters (#11–13, 16–18) with relatively small phase shifts (from 7% to15% of the cycle). Group 2a contained clusters (#3, 5–7, 15, 20) with substantial phase shifts (from 21% to 30% of the cycle), and Group 2b contained clusters (#10, #12, #19, #21, and #22) with burst middles located in almost opposite phases of the locomotor cycle during FW and BW (phase shifts from 39% to 47% of the cycle). Forty-six neurons from cluster #0 were assigned to Group 1 or Group 2 subgroups according to the value of their midburst phase shift in the FW and BW cycle. Eighteen neurons of cluster #0 fell into neither Group 1 nor Group 2 and were not further considered.

Ninety-eight of 325 modulated neurons (30%) exhibited modulation only during locomotion in one direction. Seventy-five neurons (22%) were modulated during FW only and 23 neurons (7%) were modulated during BW only (Table 2). They formed Group 3a and Group 3b, respectively. Neurons from Groups 1–3 were found in all cats (Table 2), except for Cat #3, in which Group 3b neurons were not found, most likely because of the small number of neurons ($n = 26$; Table 1) recorded in this cat.

Activity phases of Group 1–3 neurons during FW and BW

Group 1 neurons

According to the midburst phases of the clusters in the FW/BW normalized cycle (see Materials and Methods for the details), we divided all clusters forming Group 1a and Group 1b into "swing" and "stance" clusters. The mean midbursts of the swing clusters (Fig. 3*B*, white circles on crimson and violet lines; the lines show the mean cluster bursts) were located within the swing phase and at the transition from stance to swing or from swing to stance, while the mean midbursts of the stance clusters were located within the stance phase (Fig. 4).

The swing clusters (#1, #2, and #9) and stance clusters (#8 and #4), which belonged to Group 1a, contained neurons with similar phases of activity during both FW and BW (Figs. 3*B*, 4, adjacent red and blue lines, respectively), while the neurons forming Group 1b swing clusters (#13 and #18; Fig, 3*B*) and Group 1b stance clusters (#17, #14, #11, and #16; Fig. 4) had a noticeable phase shift between burst onsets during FW and BW

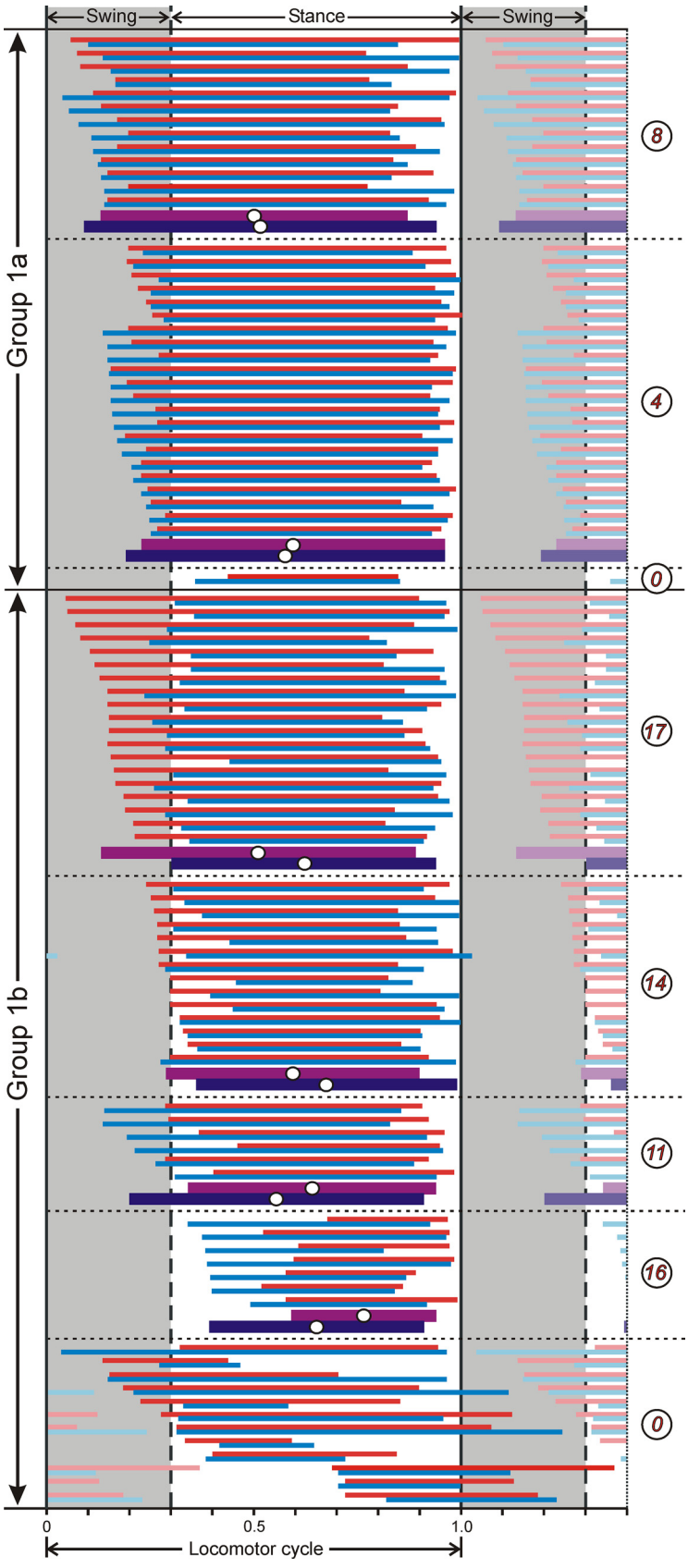

Figure 4. Phase distribution of bursts of individual Group 1 stance neurons in normalized FW/BW cycle. Abbreviations are as in Figure 3*B*.

locomotion. One can also see that phases of activity of swing clusters as well as phases of activity of stance clusters differed to some extent. Among the nine individual neurons shown in Figure 2, *A* and *B*, neurons #5 and #6 belonged to Group 1b stance and Group 1a swing populations, respectively.

Group 2 neurons

Figure 5 shows the phases of activity of individual Group 2a and Group 2b neurons during FW and BW locomotion. Each neuron in the Group 2a clusters had a long burst of activity during locomotion in one direction and a short burst of activity during locomotion in the opposite direction. A relatively small shift in the phase of the burst onsets led to a substantial overlap in the phases of activity during FW and BW locomotion in the majority of Group 2a neurons. Neurons forming clusters #20 and #7 generated a long burst during BW and a short burst during FW. By contrast, the neurons of clusters #6, #5, and #3 generated a long burst during FW and a short burst during BW. However, the phases of activity of clusters #20 and #7, as well as the phases of activity of clusters #6, #5, and #3 were noticeably different.

In general, Group 2b neurons generated a burst of activity in the opposite phases of the locomotor cycle during FW and BW. Thus, neurons forming clusters #19, #21, and #10, on average, were active in swing during FW locomotion and in stance during BW. By contrast, cluster #12 and #22 neurons were active mainly in stance during FW and in swing during BW. However, the phases of activity of clusters #19, #21, and #10, as well as the phases of activity of clusters #12 and #22 differed to some extent. Among the nine individual neurons shown in Figure 2, *A* and *B*, neurons #1 and #9 belonged to Group 2a and Group 2b, respectively.

Group 3 neurons

Figure 6, *A* and *B*, shows the phases of activity of individual Group 3a neurons during FW (Fig. 6*A*) and Group 3b neurons during BW (Fig. 6*B*). Both populations contained neurons with relatively short bursts of activity (occupying less than a half of the locomotor cycle), as well as neurons with long bursts of activity (occupying more than a half of the locomotor cycle), which are shown separately in the top and bottom parts in Figure 6, *A* and *B*, respectively. The phases of activity of the neurons with short and long bursts in both Group 3a and Group 3b were evenly distributed across the locomotor cycle (Figure 6*A*,*B*, respectively). Among the nine individual neurons shown in Figure 2, *A* and *B*, neurons #2 and #8 belonged to Group 3a.

Stability of modulation

We supposed that spinal neurons that are critically important for the control of locomotor movements in a particular direction should have

"stable" modulation. That is, they should have a small dispersion of the burst phase in the sequential locomotor cycles and the profile of their activity in individual locomotor cycles should be consistent. We used the same criteria for the stability of modulation as in the previous study (Musienko et al., 2020). (1) The SD of burst onset and/or burst offset should not be >0.1 part of the locomotor cycle (0.1 was close to the median value for all observed SDs; also, 0.1 comprised 30% of the swing phase and <20% of the stance phase; therefore an onset/offset phase with SD < 0.1 could be considered as rather precisely bound to a particular phase of the locomotor cycle). We accepted the stability of only one edge of the burst because a subset of the recorded neurons had a ramp-up or ramp-down burst shape, with stable burst offset and burst onset phases, respectively. (2) The average correlation coefficient between the profiles of the activity in individual locomotor cycles and in the entire activity histogram should not be <0.6 to ensure a consistent profile of activity in different cycles. According to these criteria, all modulated neurons were divided into the following four types: neurons with stable modulation during both FW and BW ("FW/BW-stable neurons"), neurons exhibiting stable modulation during FW only ("FW-stable neurons"), neurons exhibiting stable modulation during BW only ("BW-stable neurons"), and neurons that had unstable modulation during both FW and BW ("unstable neurons"). Among the nine individual neurons shown in Figure 2, *A* and *B*, neurons #1 and #4–6 were FW/BW-stable, while neurons #2, #3, and #8 were FW-stable. Neuron #9 was an unstable neuron.

As one can see in Figure 7*A*, the proportion of FW/BW-stable neurons in Group 1a was significantly higher than that in Groups 1b, 2a, and 2b (respectively, 43% vs 27%, 22%, and 19%; χ^2 test, $p = 0.04$, $p = 0.02$, and $p = 0.02$). In Groups 1a, 1b, and 2a, the proportions of FW-stable neurons were similar and more than twofold higher than in Group 2b (22%, 30%, and 36% vs 9%, respectively). By contrast, the proportion of BW-stable neurons was substantially higher in Group 2b compared with Groups 1a, 1b, and 2a (22% vs 6%, 15%, and 12%). The differences in the relative number of FW-stable neurons between Group 2a and Group 2b, as well as the relative number of BW-stable neurons between Group 2b and Group 1a were statistically significant (χ^2 test, $p = 0.007$ and $p = 0.03$, respectively). Finally, the proportion of unstable neurons was the highest in Group 2b (50% in Group 2 vs 29%, 25%, and 30% in Group 1a, 1b, and 2a, respectively). The differences between the relative number of unstable neurons in Group 2b and Group 1a, as well as in Group 2b and Group 1b, were statistically significant (χ^2 test, $p = 0.04$ and $p = 0.03$, respectively). In Group 3a and Group 3b, more than half of neurons were FW-stable (53%) and BW-stable (58%), respectively. The majority of clusters constituting Groups 1 and 2 contained FW/BW-stable, FW-stable, BW-stable, and unstable neurons.

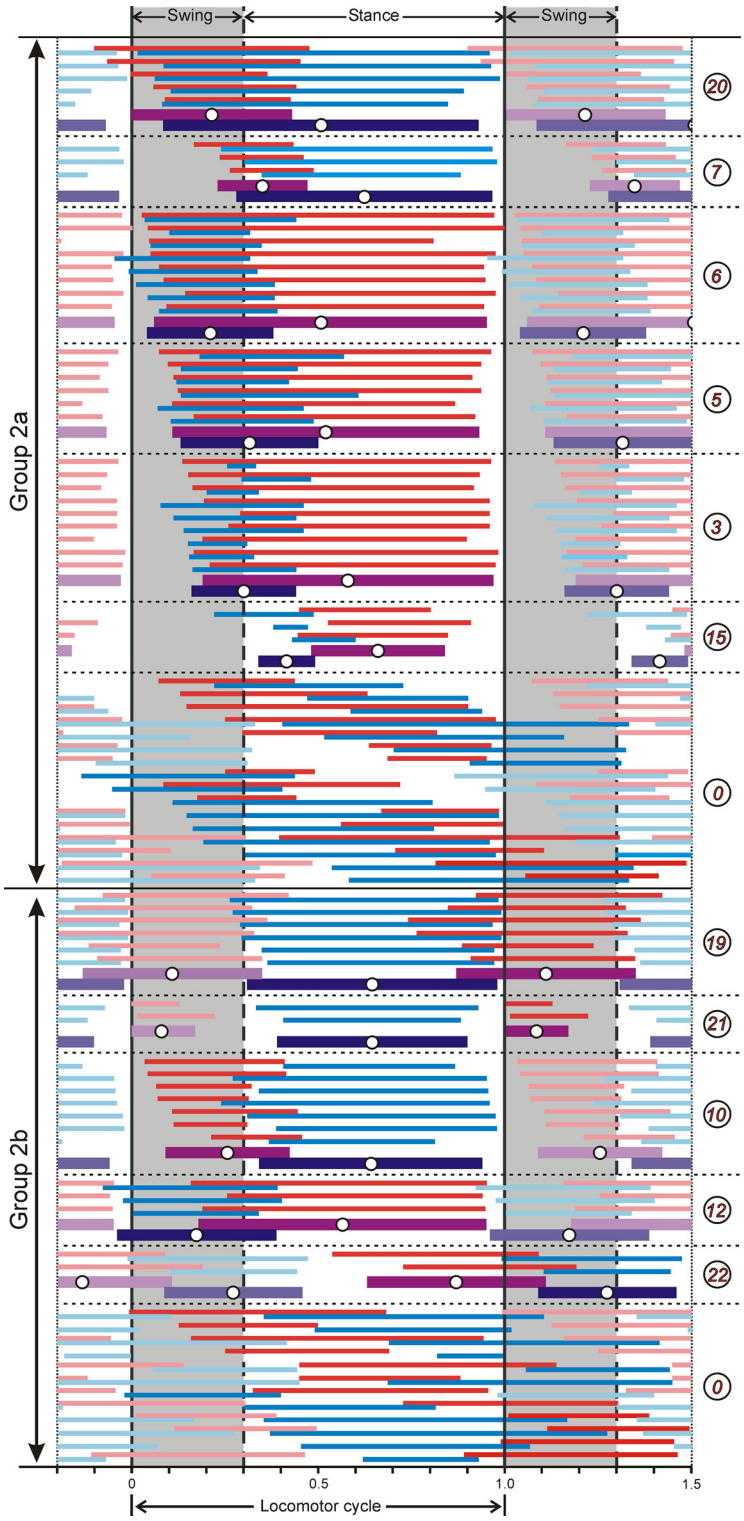

Figure 5. Phase distribution of bursts of individual Group 2a and Group 2b neurons in normalized FW/BW cycle. Abbreviations are as in Figure 3*B*.

However, it should be noted that the proportions of stable neurons in Groups 1–3 revealed in the present study, were most likely underestimated because most neurons modulated during ES-

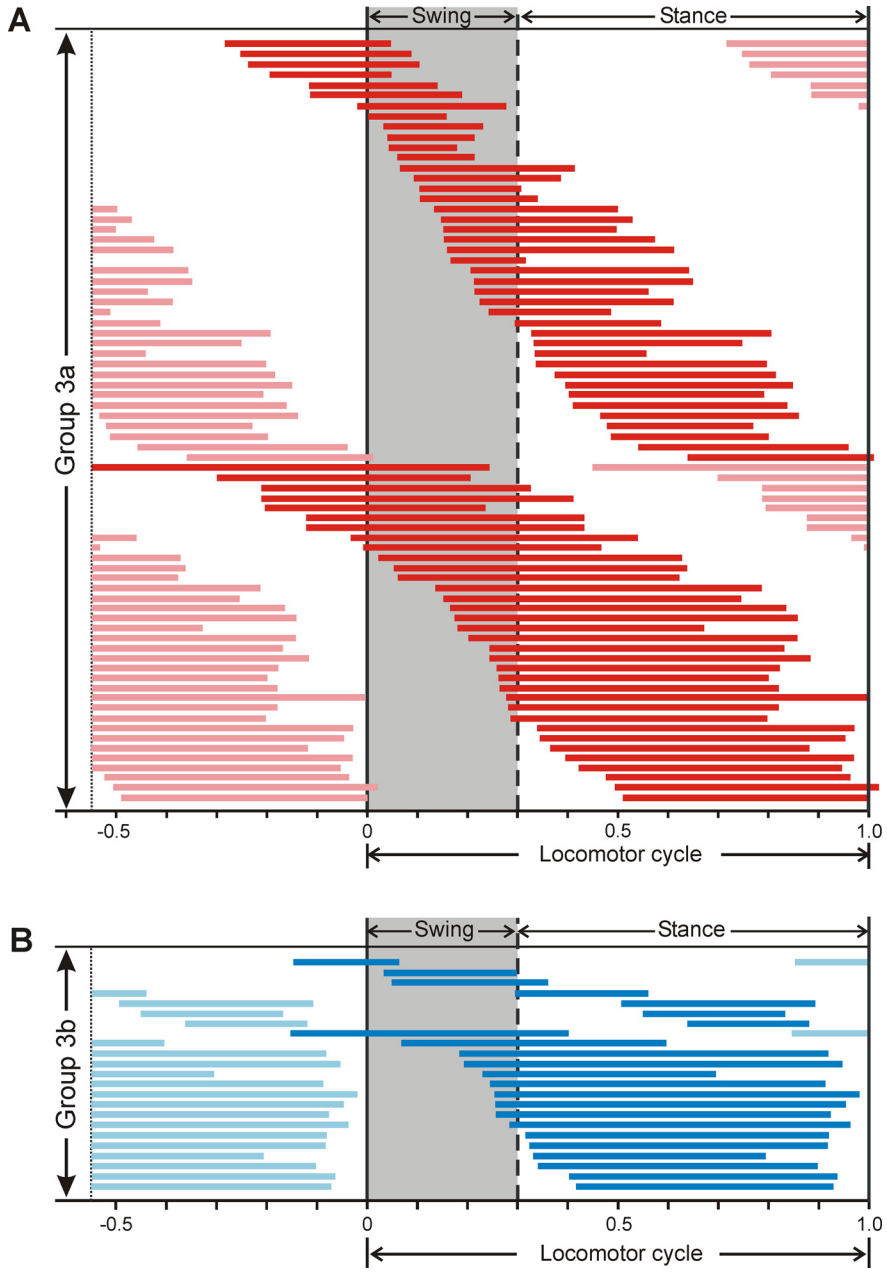

Figure 6. Phase distribution of Group 3 neurons. ***A***, ***B***, Distribution of bursts of individual Group 3a (***A***) and Group 3b (***B***) neurons in normalized FW/BW cycle, respectively. Abbreviations are as in Figure 3*B*. Phase distribution of neurons with "short" and "long" bursts of activity are shown separately.

evoked locomotion respond to individual ES stimulus (Deliagina et al., 2017), which affects the stability of their modulation. We demonstrated that a substantial proportion of individual spinal neurons exhibiting stable modulation during FW evoked by supraspinal commands showed unstable modulation during ES-evoked FW (Musienko et al., 2020).

Distribution of Groups 1–3 neurons in the spinal cord

Figure 8*A–D* shows the location of individual neurons from different populations of Groups 1–3 recorded in L4, L5, and L6 on the corresponding cross sections of the spinal cord. One can see that most of these neurons were recorded in the intermediate and ventral parts of the gray matter outside the area of motor nuclei (Vanderhorst and Holstege, 1997), and were, thus, considered putative interneurons. The neurons of different groups were intermixed.

Group 1–3 neurons were not evenly distributed in the L4–L6 segments (Fig. 7*B*). Thus, Group 1 neurons dominated and constituted about half of all recorded neurons in L5 and L6 (51% and 45%, respectively). The difference in the relative number of Group 1 neurons recorded in L4 and L5 was statistically significant (30% vs 51%; χ^2 test, $p = 0.01$). Although the proportion of Group 3 neurons was slightly higher in L4 (40%) compared with that in L5 (32%) and L6 (27%), the difference was insignificant. The proportion of Group 2 neurons in L5 was substantially lower than that in L4 and L6 (17% vs 30% and 29%, respectively). The difference in the relative number of Group 2 neurons recorded in L5 and L4 was statistically significant (χ^2 test, $p = 0.047$).

The specific populations of neurons within each of three groups were also not evenly distributed in the L4–L6 segments (Fig. 7*B*). Thus, while similar proportions of Group 1a and Group 1b swing neurons were recorded in L5 and L6 segments, in the L4 segment, Group 1b swing neurons were absent. The proportion of Group 1 stance neurons did not differ significantly from the proportion of Group 1 swing neurons in L5 (31% vs 21%; χ^2 test, $p = 0.08$), but in L4 and L6, the proportion of Group 1 stance neurons was significantly higher than that in Group 1 swing neurons (23% vs 8% and 29% vs 15%, respectively; χ^2 test, $p = 0.03$ and $p = 0.002$, respectively). Within the Group 1 stance population, the proportion of Group 1a stance neurons in L6 was similar to that in L5 (14% and 10%, respectively), but it was significantly lower than that in L4 (14% vs 4%; χ^2 test, $p = 0.04$). The relative number of Group 2b neurons recorded in L5 was similar to that in L4 (5% and 7%, respectively), but it was significantly lower than that recorded in L6 (5% vs 14%; χ^2 test, $p = 0.02$). Finally, the highest proportion of Group 3b neurons was recorded in L4 (17% vs 3% and 7% in L5 and L6, respectively; χ^2 test, $p = 0.002$ and $p = 0.02$, respectively).

Activity levels of neurons in Groups 1–3 during FW and BW

Figure 9*A–E* compares various activity characteristics [the mean ± SD values of spontaneous activity (Fig. 9*A*), cycle frequency (Fig. 9*B*), burst frequency (Fig. 9*C*), interburst frequency (Fig. 9*D*), and coefficient of modulation (Fig. 9*E*)] during FW and BW for different populations of Groups 1–3. Neurons in Group 2a and Group 2b were pooled since the levels of spontaneous activity and all parameters of activity during FW, as well as during BW, were similar.

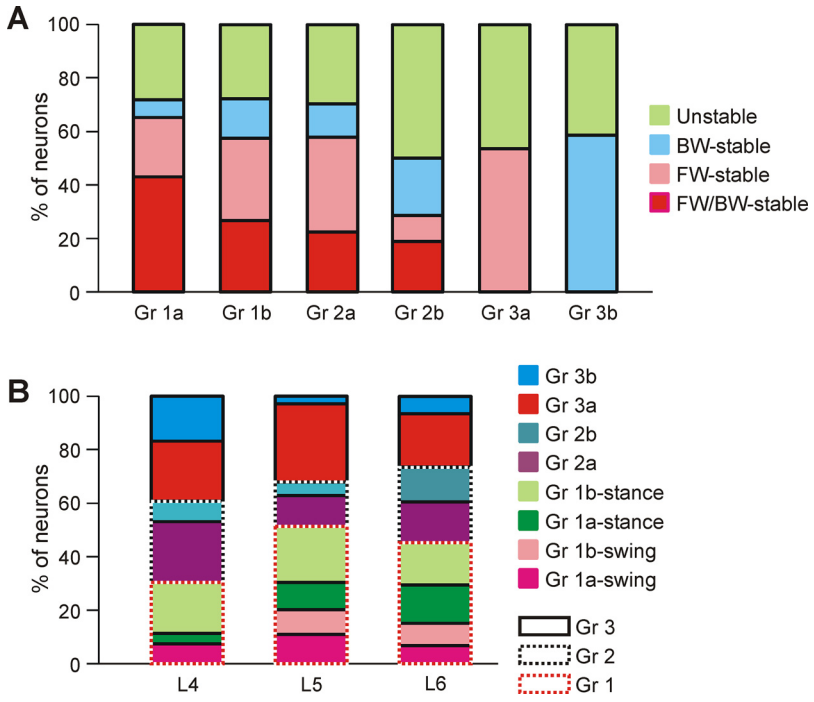

Figure 7. Distribution of different populations of Group 1–3 neurons in L4–L6 and the stability of their modulation during FW and BW. ***A***, Relative number of FW/BW-stable, FW-stable, BW-stable, and unstable neurons within different populations of Group 1–3 neurons. ***B***, Proportion of different populations in Group 1–3 neurons recorded in L4, L5, and L6. In ***B***, Group 1, Group 2, and Group 3 are outlined by dotted red, dotted black, and solid black lines, respectively. Gr, Group.

In general, the mean values of spontaneous activity as well as the mean values of cycle frequency, burst, and interburst frequency during FW, were similar in most populations of Group 1–3 neurons. Also, in most populations, the activity parameters during FW did not differ significantly from those during BW. However, there were a few exceptions. Thus, the mean value of spontaneous activity (Fig. 9*A*) in Group 3b neurons was almost fivefold lower compared with those in Group 1 (1.26 ± 2.48 vs 7.05 ± 8.54 Hz; unpaired *t* test, $t_{(125)} = 6.64$, $p = 8.5 \times 10^{-10}$), Group 2 (1.26 ± 2.48 vs 6.22 ± 7.58 Hz; unpaired *t* test, $t_{(103)} = 5.07$, $p = 1.8 \times 10^{-6}$), and Group 3a neurons (1.26 ± 2.48 vs 6.69 ± 10.79 Hz; unpaired *t* test, $t_{(92)} = 4.04$, $p = 0.0001$). The value of the mean interburst frequency (Fig. 9*D*) in Group 1a swing neurons during BW was twofold higher than that during FW (respectively, 15.19 ± 17.82 vs 6.48 ± 7.68 Hz; paired *t* test, $t_{(26)} = -3.80$, $p = 7.9 \times 10^{-4}$) and twofold higher than that in Group 3b neurons (15.19 ± 17.82 vs 7.31 ± 8.35 Hz; unpaired *t* test, $t_{(38)} = -2.06$, $p = 0.046$). Small but significant differences were also found between the mean burst frequencies (Fig. 9*C*) in Group 1a swing neurons and Group 1a stance neurons during BW locomotion (respectively, 41.21 ± 28.86 vs 28.75 ± 15.00 Hz; unpaired *t* test, $t_{(36)} = 2.05$, $p = 0.048$), in Group 1a swing neurons and Group 3a neurons during FW (respectively, 26.96 ± 20.13 vs 38.18 ± 24.44 Hz; unpaired *t* test, $t_{(39)} = -2.14$, $p = 0.04$), in Group 1b swing neurons during FW and BW (respectively, 35.25 ± 21.10 vs 30.72 ± 20.40 Hz; paired *t* test, $t_{(23)} = 2.20$, $p = 0.04$), as well as between the mean interburst frequencies (Fig. 9*D*) during BW in Group 2 and Group 3b neurons (respectively, 12.50 ± 12.27 vs 7.31 ± 8.36 Hz; unpaired *t* test, $t_{(55)} = -2.38$, $p = 0.02$).

In contrast to the parameters of activity considered above, which were similar during FW and BW in most populations of Group 1–3 neurons, the value of the coefficient of modulation (Fig. 9*E*) in the majority of Group 1–3 populations was significantly decreased during BW compared with that during FW [respectively: $69 \pm 21\%$ vs $85 \pm 12\%$ in Group 1a swing population (paired *t* test, $t_{(26)} = 5.41$, $p = 1.13 \times 10^{-5}$); $62 \pm 20\%$ vs $74 \pm 19\%$ in Group 1a stance population (paired *t* test, $t_{(70)} = 2.67$, $p = 0.0095$); $70 \pm 19\%$ vs $77 \pm 18\%$ in Group 1b stance population (paired *t* test, $t_{(114)} = 2.08$, $p = 0.04$); $66 \pm 19\%$ vs $71 \pm 20\%$ in Group 2 neurons (paired *t* test, $t_{(81)} = 2.29$, $p = 0.02$)]. Also, during FW, the coefficient of modulation in Group 1a swing neurons was significantly higher than that in each of other populations of Group 1–3 neurons [$85 \pm 12\%$ vs $67 \pm 23\%$ in Group 1b swing neurons, $74 \pm 19\%$ in Group 1a stance neurons, $77 \pm 18\%$ in Group 1b stance neurons, $71 \pm 20\%$ in Group 2 neurons, $74 \pm 20\%$ in Group 3a neurons; unpaired *t* test, respectively: $t_{(35)} = 3.41$, $p = 0.002$; $t_{(60)} = 2.68$, $p = 0.0095$; $t_{(70)} = 2.40$, $p = 0.02$; $t_{(71)} = 4.42$, $p = 3.4 \times 10^{-5}$; $t_{(74)} = 3.35$, $p = 0.001$) while during BW, a significant difference was found only between the values of the coefficient of modulation in Group 3b and Group 1a stance neurons ($74 \pm 19\%$ vs $62 \pm 20\%$; unpaired *t* test, $t_{(50)} = 2.29$, $p = 0.03$).

The characteristics of activity in Group 1–3 neurons during FW were similar to those during ES-evoked FW reported in our previous study (Musienko et al., 2020).

Contribution of sensory feedback observed in a quiescent state to the modulation of individual Group 1–3 neurons during FW and BW

Although changes in the processing of specific types of afferent signals from the limbs during FW compared with that in the quiescent state have been demonstrated (Duysens and Pearson, 1980; Conway et al., 1987; Shefchyk et al., 1990; Gossard et al., 1994; McCrea, 1998; Quevedo et al., 1998; Angel et al., 2005), one cannot exclude the existence of a neuronal population the modulation of which is determined by sensory feedback, with processing similar to that observed in a quiescent state. To reveal such neurons, more than half of Group 1–3 neurons ($n = 91$, 22, 14, 47, and 14 from Group 1, Group 2a, Group 2b, Group 3a, and Group 3b, respectively) were recorded during both passive movements of the ipsilateral hindlimb and passive movements of the contralateral hindlimb performed along both the FW and BW trajectories (see Materials and Methods). We did not find substantial differences between data related to different populations of Group 1 neurons, and they were therefore pooled.

Figure 10*A–D* shows the relative number of neurons with different responses to passive limb movements in different populations of Group 1–3 neurons. One can see that, in each population, the overwhelming majority of neurons was modulated by movements of at least one of the hindlimbs along the FW trajectory, as well as along the BW trajectory (Fig. 10, Ip- & Co-, Ip-, Co-). Also, in Group 1, Group 2a, Group 2b, and Group 3a, the relative number of neurons modulated by movements of the ipsilateral limb and the contralateral limb (Fig. 10,

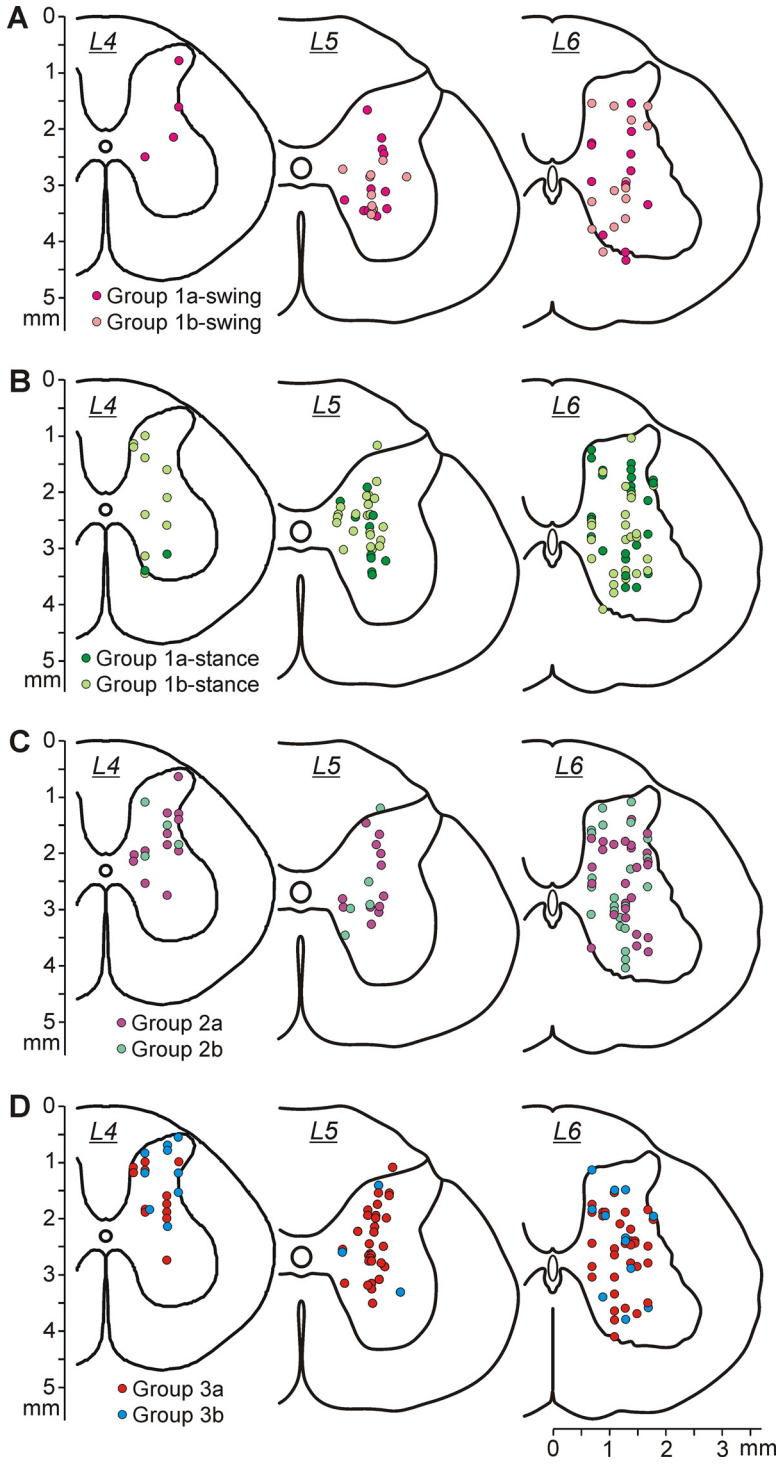

Figure 8. Group 1–3 neurons recorded in L4, L5, and L6 spinal segments during both FW and BW. ***A–D***, Positions of Group 1a and Group 1b swing neurons (***A***), Group 1a and Group 1b stance neurons (***B***), as well as Group 2a and Group 2b neurons (***C***), and Group 3a and Group 3b neurons (***D***) on the cross section of the spinal cord, recorded in L4, L5, and L6.

Ip- & Co-), as well as the relative number of neurons modulated by movements of the ipsilateral limb only (Fig. 10, Ip-), were substantially higher than the number modulated by movements of the contralateral limb only (Fig. 10, Co-). In Group 3b, the proportion of neurons modulated by movements of the ipsilateral hindlimb only was also much higher than that modulated by movements of the contralateral hindlimb only; however, the proportion of neurons modulated by movements of the ipsilateral limb and the contralateral limb was twofold lower compared with that modulated by movements of the contralateral limb only (Fig. 10*D*, 7% vs 14%, respectively). In general, the proportions of neurons modulated by sensory inputs from both limbs, from the ipsilateral limb only, and from the contralateral limb only, as revealed by FW and BW movements, were similar in Groups 1, 2a, and 2b.

The populations of Group 1–3 neurons differed in the proportion of neurons for which modulation during FW and BW locomotion could be explained by the sensory feedback from the limbs observed in a quiescent state. Thus, in Group 2b, Group 3a, and Group 3b, the proportion of such neurons was substantially higher than that in Group 1 and Group 2a [for FW: 31% in Group 2b vs 5% in Group 1 (χ^2 test, $p = 0.002$), 31% in Group 2b vs 5% in Group 2a (χ^2 test, $p = 0.03$), 34% in Group 3a vs 5% in Group 1 (χ^2 test, $p = 9.7 \times 10^{-6}$), 34% in Group 3a vs 5% in Group 2a (χ^2 test, $p = 0.007$); for BW: 15% in Group 2b vs 3% in Group 1, 15% in Group 2b vs 5% in Group 2a, 21% in Group 3b vs 3% in Group 1 (χ^2 test, $p = 0.007$), 21% in Group 3b vs 5% in Group 2a]. In contrast, the relative number of neurons in which sensory feedback observed in a quiescent state could potentially contribute to locomotor modulation was substantially lower in Group 3a and Group 3b compared with those in Group 1 and Group 2a [for FW: 13% in Group 3a vs 46% in Group 1 (χ^2 test, $p = 9.5 \times 10^{-5}$), 13% in Group 3a vs 50% in Group 2a (χ^2 test, $p = 0.0008$); for BW: 14% in Group 3b vs 49% in Group 1 (χ^2 test, $p = 0.009$), 14% in Group 3b vs 45% in Group 2a (χ^2 test, $p = 0.04$)]. In Group 2b neurons, for FW the proportion of such neurons was twofold lower (23%) than that for BW (23% vs 46%).

However, it is necessary to note that passive limb movement along the locomotor trajectory only partly mimicked the sensory feedback during real locomotion. One may expect that many limb afferents were activated similarly during passive and locomotor limb movement (e.g., joint afferents, mechanoreceptors of the foot sole), while other afferents most likely had weaker activity (e.g., muscle spindle afferents that have central control mediated by γ-motoneurons; Murphy et al., 1984) or were silent (e.g., Ib afferents). One cannot also rule out the possibility that the level of excitability of spinal networks in decerebrate preparation is lower than that in the quiescent state of intact subjects. Thus, one cannot exclude that the proportion of neurons for which modulation is

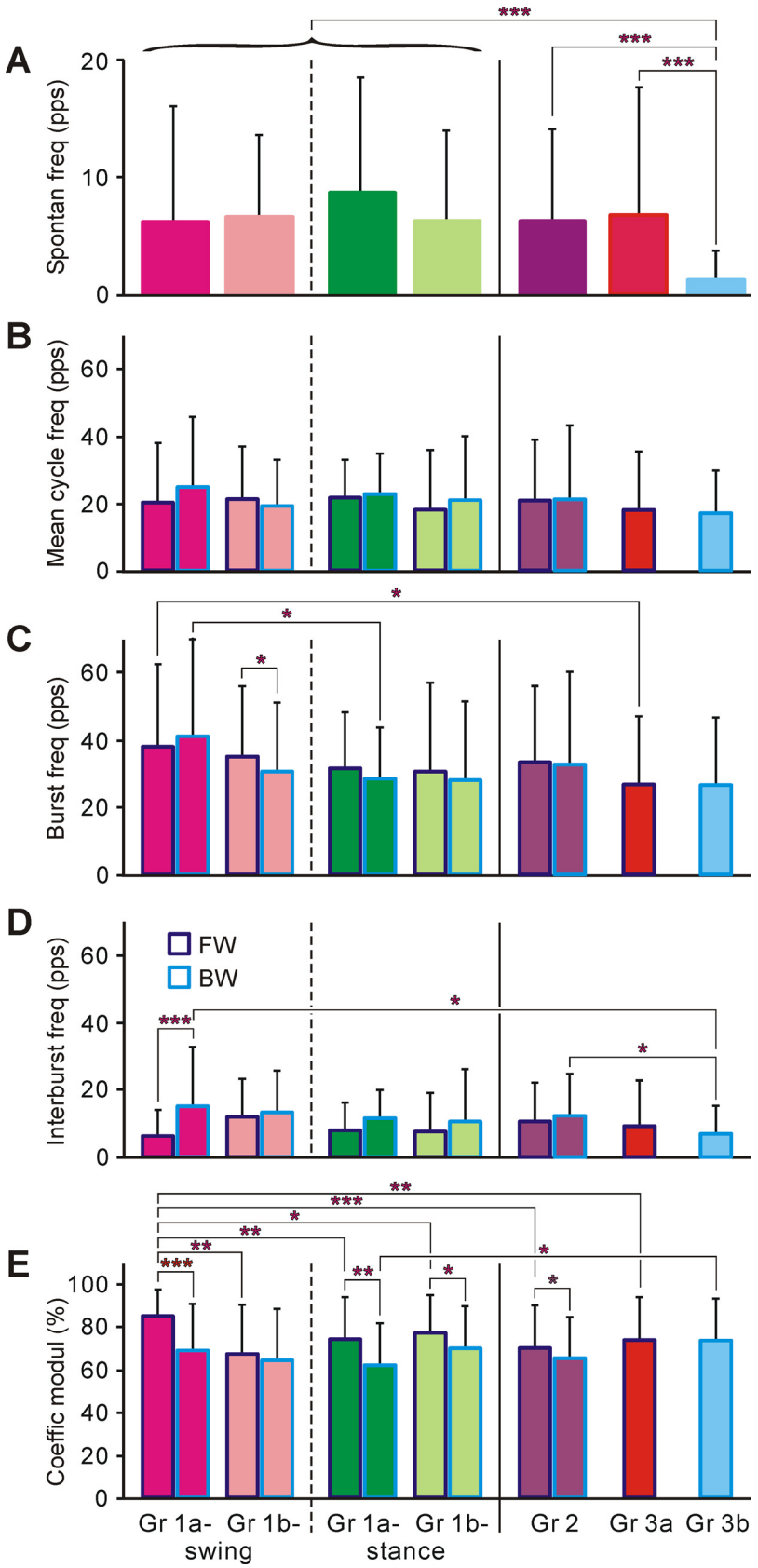

Figure 9. Comparison of different parameters of activity in different populations of Group 1–3 neurons during FW and BW. ***A–E***, Mean ± SD values of spontaneous frequency (***A***), cycle frequency (***B***), burst frequency (***C***), and interburst frequency (***D***), and coefficient of modulation (***E***) for Group 1a and Group 1b swing, Group 1a and Group 1b stance, Group 2, Group 3a, and Group 3b neurons during FW (bars outlined by violet) and BW (bars outlined by blue). The number (*N*) of animals and the number (*n*) of Group 1a swing, Group 1b swing, Group 1a stance, Group 1b stance, Group 2, Group 3a, and Group 3b neurons are as follows: $N = 4$, and $n = 27, 24, 36, 58, 82, 75$, and 23, respectively. $^{*}p < 0.05$, $^{**}0.001 < p < 0.01$, $^{***}p < 0.001$.

determined by sensory feedback, with processing similar to that observed in a quiescent state, was underestimated.

Discussion

In the present study, we compared the activity of the same individual spinal neurons during real (with normal sensory feedback from limbs) FW and BW evoked in decerebrate cats by ES of the spinal cord. We found that most neurons modulated their activity during FW and/or BW, suggesting that they contribute to the control of stepping. Among the modulated neurons, we revealed and characterized three groups of neurons that differed in their activity phases during FW and BW.

Individual neurons in Group 1 had similar activity phases during both FW and BW and thus, form a part of the locomotor network operating similarly under both conditions. We suggest that it generates a vertical component of steps (the limb elevation and lowering; Fig. 11*A*) exhibited during stepping in any direction. Group 1a neurons, in which the activity phases are almost identical during FW and BW, may form the rhythm-generating part of this network. Clusters with different phases likely play different functional roles in the control of the vertical component of steps, e.g., clusters #1, #2, and #9 from Group 1a swing generate, respectively, elevation, the limb maintenance above the ground during swing, and the limb lowering, while clusters #4 and #8 from Group 1a stance generate, respectively, limb lowering and the maintenance of the limb on the ground (Fig. 11*B*).

In contrast to Group 1 neurons, Group 2 neurons had substantially different activity phases during FW and BW. Thus, Group 2 neurons form a part of the locomotor network that changes its operation with a change in stepping direction. Among Group 2b neurons, bursts of activity during FW and BW were almost in antiphase. Because the main kinematic difference between BW and FW is reversed hip joint motion (Buford et al., 1990), Group 2b neurons likely control the direction of the hip motion. Clusters #10, #19, and #21 (active during FW swing and BW stance) cause hip flexion, while clusters #12 and #22 (active during FW stance and BW swing) evoke hip extension. Thus, we suggest that Group 2b neurons belong to

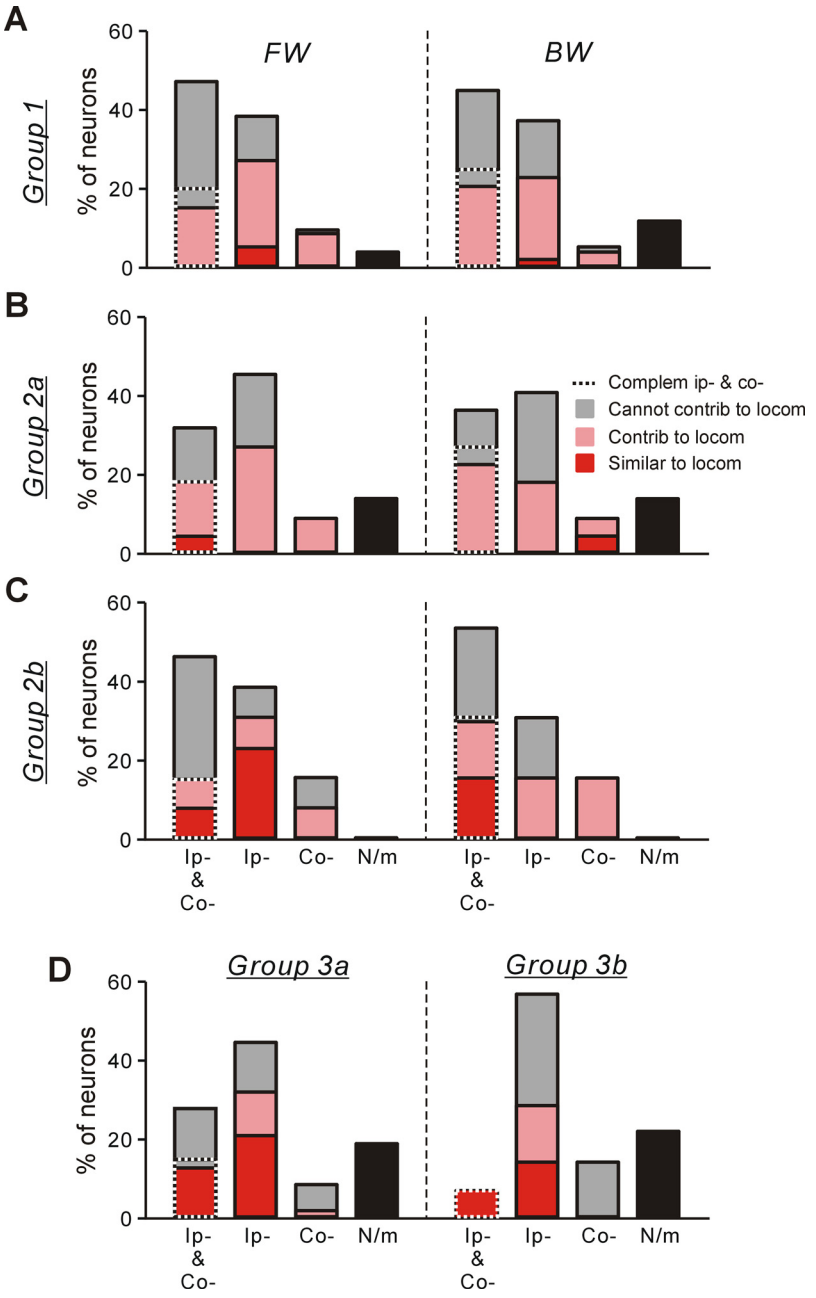

Figure 10. Effects of passive movements of the ipsilateral and the contralateral hindlimbs along the FW and BW trajectory on the activity of neurons in different populations of Groups 1–3. ***A–D***, Relative numbers of neurons modulated by passive movements of either hindlimb (Ip- and Co- bars), neurons modulated by movements of only ipsilateral or only contralateral limb (Ip- and Co- bars, respectively), and neurons nonmodulated by passive limb movements (*N*/*m* bars), in populations of Group 1 (***A***), Group 2a (***B***), Group 2b (***C***), Group 3a (***D***), and Group 3b (***D***) neurons. Parts of the Ip- & Co- bars with dotted and solid outlines show the proportions of neurons with complimentary (Complem Ip- & Co-) and opposite inputs from ipsilateral and contralateral hindlimb (see Materials and Methods for explanation), respectively. Red, pink, and gray parts of the bars indicate the proportion of neurons with the phase of modulation caused by sensory feedback similar to, strongly overlapping with, and different from that observed during locomotion (Similar to locom, Contrib to locom, and Cannot contrib to locom, respectively). The number (*N*) of animals, and the number (*n*) of Group 1, Group 2a, Group 2b, Group 3a, and Group 3b neurons are as follows: $N = 4$, $n = 91$, 22, 14, 47, and 14, respectively.

the mechanism generating the horizontal component of the step (Fig. 11*A*,*C*).

In Group 2a neurons, the burst onset phases (in late swing) were almost identical during FW and BW. However, during locomotion in one direction the burst was short (terminated in early stance), while during locomotion in the opposite direction it occupied almost the entire stance. We assume that clusters #3, #5, and #6 and clusters #7 and #20, respectively, contribute to limb lowering during both FW and BW but to the generation of the propulsive force only during FW and BW (Fig. 11*A*,*C*). Thus, Group 2a contributes to the control of both the vertical and horizontal components of steps.

Finally, the activity of Group 3 neurons is modulated during FW only (Group 3a) or BW only (Group 3b), suggesting that they belong to the networks determining the forward or backward direction of stepping, respectively (Fig. 11*A*,*C*).

We found that the proportion of FW/BW-stable neurons is significantly higher in Groups 1a and 3 compared with Groups 1b and 2. Potentially, Group 1a FW/BW-stable neurons form the core of the rhythm-generating locomotor network, while Group 3a FW-stable neurons and Group 3b BW-stable neurons are critically important for the control of the forward and backward direction of stepping, respectively.

We did not find any substantial differences between activity parameters in Group 1–3 neurons, as well as between activity parameters during FW and BW in specific Group 1 and 2 populations. The only significant, though rather small, difference was found in the coefficient of modulation, which was decreased during BW in most Group 1 and 2 populations. This could be related to the smaller amplitude of the limb movements during BW compared with FW (Musienko et al., 2012; Merkulyeva et al., 2018; Fig. 1*B–D*).

We found that, although most neurons were modulated by passive locomotor-like movements of the ipsilateral and/or contralateral hindlimb, the FW/BW-related modulation of most Group 1–3 neurons was not determined by the sensory feedback from the limbs observed in a quiescent state. These results confirm those of our previous study devoted to FW (Musienko et al., 2020) and are in line with earlier studies (Duysens and Pearson, 1980; Conway et al., 1987; Shefchyk et al., 1990; Gossard et al., 1994; McCrea, 1998; Quevedo et al., 1998; Angel et al., 2005). Also, our results suggest that, when activated, not only forward but also backward locomotor networks strongly modify the observed at rest sensory inputs from the limbs to most spinal neurons. Nevertheless, Groups 2b and 3 had significantly higher proportions of neurons with locomotor modulation that can be explained by sensory feedback observed during passive limb movements than Groups 1 and 2a. Because the networks generating the horizontal component of steps are driven by the sensory feedback from limbs (Musienko et al., 2012), this result supports our suggestion that Group 2b and 3 neurons are elements of these networks.

There are two main conceptual models of the organization of locomotor networks. The two-layer hypothesis (McCrea and Rybak, 2008; Rybak et al., 2015) suggests that the network contains a central rhythm generator, which drives the pattern formation layer. By contrast, the one-layer hypothesis (Grillner, 2006; Grillner and Kozlov, 2021) suggests that the network consists of a set of "unit burst generators" controlling groups of synergistic muscles at different joints, while changed interactions between them result in the generation of different locomotor patterns, including FW and BW. Our results are compatible with both these models. One can suggest that, in the framework of the two-layer hypothesis (McCrea and Rybak, 2008; Rybak et al., 2015), Group 1a neurons belong to the rhythm-generating layer, and Groups 1b, 2, and 3 neurons belong to the pattern formation layer, while in the framework of the one-layer hypothesis (Grillner, 2006; Grillner and Kozlov, 2021), Group 1 neurons form unit burst generators and Group 2 and 3 neurons coordinate the unit burst generators shaping the locomotor pattern.

We suggest that the four interneuronal populations (Groups 1, 2, 3a, and 3b) form four modules of the locomotor network, which can be selectively activated in a specific combination to generate stepping in a particular direction or in place. Also, we demonstrated that operation of the Group 2 module changes with a change in stepping direction. The modular organization of the locomotor network controlling swimming speed was demonstrated in adult zebrafish (Ampatzis et al., 2014). Several findings in mice (Talpalar et al., 2013; Rancic et al., 2020; Falgairolle and O'Donovan, 2021; Zelenin et al., 2021), cats (Krouchev et al., 2006; Desrochers et al., 2019), and humans (Huang et al., 2021; Yokoyama et al., 2021) also point to the modular organization of the network generating different locomotor patterns.

Recent advances in genetics have inspired numerous studies striving to identify the components of spinal locomotor networks based on transcription factor expression (Kiehn, 2016; Rancic and Gosgnach, 2021). Although no single genetically identified type of spinal neurons has been found to be solely responsible for rhythm generation or the control of step direction, there is evidence that Shox2 non-V2a neurons and Hb9 interneurons may contribute to the generation of locomotor rhythmic activity (Dougherty et al., 2013; Kiehn, 2016; Caldeira et al., 2017). The present study and other studies (Talpalar et al., 2013; Rancic et al., 2020; Falgairolle and O'Donovan, 2021; Zelenin et al., 2021) suggest that different locomotor patterns are generated by specific combinations of modules of the locomotor network and, moreover, that the operation of some modules can be remarkably changed with a change in the generated pattern. Thus, the functional role of a genetically identified neuronal population in the control of locomotor movements can depend on the type of locomotor pattern generated, and therefore, results obtained in *in vitro* preparations generating a "locomotor-like" motor pattern should be considered with caution.

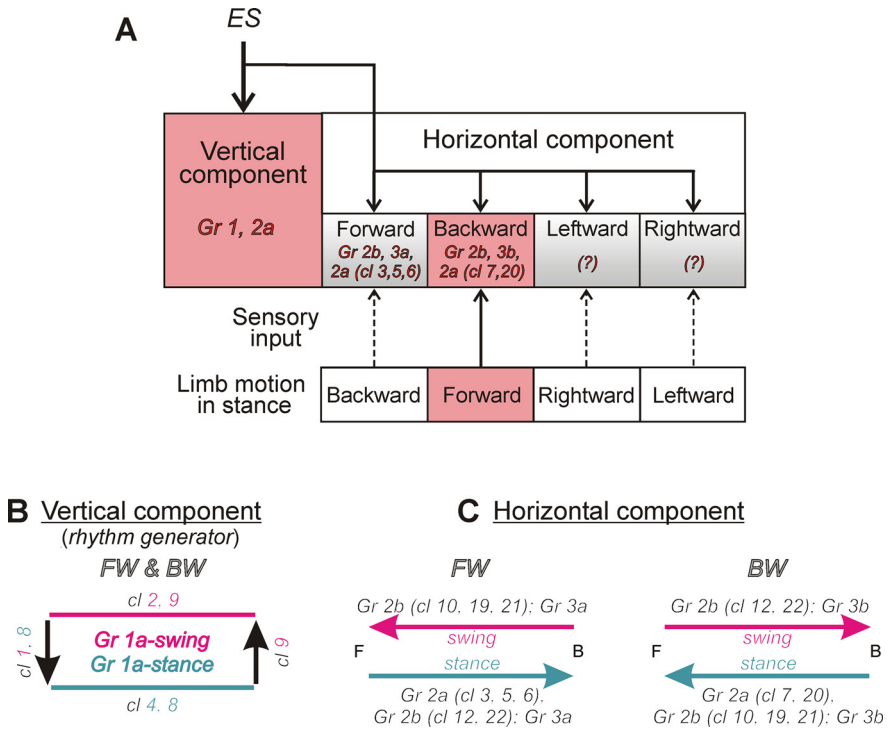

Figure 11. Hypothetical contribution of different groups of spinal neurons to the generation of the vertical and horizontal components of the step. ***A***, Basic mechanisms for the control of step direction (modified from Musienko et al., 2012). ES of the spinal cord activates a network generating a vertical component of step. It also causes subthreshold activation of all networks generating a horizontal component. Because of the treadmill motion (e.g., forward), the limb reaches the extreme anterior position, and sensory feedback activates network backward, resulting in the backward step. Thus, ES evokes stepping opposite to the direction of treadmill motion. Neuronal Groups (Gr) and their clusters (cl) that presumably contribute to generation of the vertical component of step, as well as the horizontal forward and backward components of step are indicated. ***B***, Group 1a clusters, presumably contributing to the generation of different phases of vertical component of the step. The limb elevation, maintenance of the limb in an elevated position during swing, the limb lowering, and maintenance of the limb in a lowered position are indicated by upward black arrow, crimson horizontal line, downward black arrow, and green horizontal line, respectively. Crimson and green numbers indicate clusters that belong to Group 1a swing and Group 1a stance, respectively. ***C***, Neuronal groups as well as specific clusters of Group 2b and Group 2a neurons, presumably contributing to the generation of different phases of the horizontal component of the step during FW and BW. Crimson and green arrows show direction (F, forward; B, backward) of the limb movement in relation to the trunk during swing and stance, respectively.

Because there are some differences in FW and BW kinematics evoked by ES in decerebrate cats (Musienko et al., 2012, 2020; Merkulyeva et al., 2018) and by supraspinal command in intact cats (Buford et al., 1990; Buford and Smith, 1990), one could suppose that different locomotor networks are activated in these two conditions. However, recently, we demonstrated that the same locomotor network generates FW caused by ES and stimulation of the mesencephalic locomotor region. Slightly distorted during ES operation of a part of this network can explain some differences in FW kinematics observed in the two conditions (Musienko et al., 2020). Thus, the same locomotor modules generating BW are likely activated by ES and a specific supraspinal command in intact animals, and slight differences in operation of some modules lead to differences in kinematics. Unfortunately, the brain center for initiation of BW is unknown, and this assumption cannot be tested experimentally.

To conclude, in the present study for the first time, the operation of spinal locomotor networks during real FW and BW evoked by ES of the spinal cord has been compared at the level of individual spinal interneurons. Neuronal groups potentially

forming four parts (modules) of the locomotor network generating the vertical and horizontal components of the forward and backward steps have been revealed and characterized. The obtained results support our previously formulated hypothesis about the functional organization of the locomotor network generating stepping in different directions and provide new insights into the understanding of its operation. Also, these results advance our understanding of the neuronal mechanisms of therapeutic ES effects and can potentially be used for the development of novel strategies for recuperation of both locomotor function and balance control, which requires the generation of corrective steps in different directions.

References

Ampatzis K, Song J, Ausborn J, El Manira A (2014) Separate microcircuit modules of distinct v2a interneurons and motoneurons control the speed of locomotion. Neuron 83:934–943.

Angel MJ, Jankowska E, McCrea DA (2005) Candidate interneurones mediating group I disynaptic EPSPs in extensor motoneurones during fictive locomotion in the cat. J Physiol 563:597–610.

Ashley-Ross MA, Lauder GV (1997) Motor patterns and kinematics during backward walking in the Pacific Giant Salamander: evidence for novel motor output. J Neurophysiol 78:3047–3060.

Batschelet E (1981) Circular statistics in biology. New York: Academic.

Beloozerova IN, Zelenin PV, Popova LB, Orlovsky GN, Grillner S, Deliagina TG (2003) Postural control in the rabbit maintaining balance on the tilting platform. J Neurophysiol 90:3783–3793.

Berkowitz A, Stein PS (1994) Activity of descending propriospinal axons in the turtle hindlimb enlargement during two forms of fictive scratching: phase analyses. J Neurosci 14:5105–5119.

Buford JA, Smith JL (1990) Adaptive control for backward quadrupedal walking. II. Hindlimb muscle synergies. J Neurophysiol 64:756–766.

Buford JA, Zernicke RF, Smith JL (1990) Adaptive control for backward quadrupedal walking. I. Posture and hindlimb kinematics. J Neurophysiol 64:745–755.

Caldeira V, Dougherty KJ, Borgius L, Kiehn O (2017) Spinal Hb9::Cre-derived excitatory interneurons contribute to rhythm generation in the mouse. Sci Rep 7:41369.

Conway BA, Hultborn H, Kiehn O (1987) Proprioceptive input resets central locomotor rhythm in the spinal cat. Exp Brain Res 68:643–656.

Courtine G, Gerasimenko Y, Brand R, Yew A, Musienko P, Zhong H, Song B, Ao Y, Ichiyama RM, Lavrov I, Roy RR, Sofroniew MV, Edgerton VR (2009) Transformation of nonfunctional spinal circuits into functional states after loss of brain input. Nat Neurosci 12:1333–1342.

Deliagina TG, Musienko PE, Gorskii OV, Lyalka VF, Merkulyeva N, Gerasimenko YP, Zelenin PV (2017) Spinal neurons mediating effect epidural stimulation of the spinal cord on locomotor network. Soc Neurosci Abstr 43:065.09.

Deliagina TG, Musienko PE, Zelenin PV (2019) Nervous mechanisms of locomotion in different directions. Curr Opin Physiol 8:7–13.

Desrochers E, Harnie J, Doelman A, Hurteau M-F, Alain Frigon A (2019) Spinal control of muscle synergies for adult mammalian locomotion. J Physiol 597:333–350.

Dougherty KJ, Zagoraiou L, Satoh D, Rozani I, Doobar S, Arber S, Jessell TM, Kiehn O (2013) Locomotor rhythm generation linked to the output of spinal shox2 excitatory interneurons. Neuron 80:920–933.

Duysens J, Pearson KG (1980) Inhibition of flexor burst generation by loading ankle extensor muscles in walking cats. Brain Res 187:321–332.

Eilam D, Shefer G (1992) Reversal of interleg coupling in backward locomotion implies a prime role of the direction of locomotion. J Exp Biol 173:155–163.

Falgairolle M, O'Donovan MJ (2021) Optogenetic activation of V1 interneurons reveals the multimodality of spinal locomotor networks in the neonatal mouse. J Neurosci 41:8545–8561.

Forssberg H, Grillner S, Halbertsma J, Rossignol S (1980) The locomotion of the low spinal cat. II. Interlimb coordination. Acta Physiol Scand 108:283–295.

Frigon A, Desrochers É, Thibaudier Y, Hurteau MF, Dambreville C (2017) Left-right coordination from simple to extreme conditions during split-belt locomotion in the chronic spinal adult cat. J Physiol 595:341–361.

Gerasimenko Y, Musienko P, Bogacheva I, Moshonkina T, Savochin A, Lavrov I, Roy RR, Edgerton VR (2009) Propriospinal bypass of the serotonergic system that can facilitate stepping. J Neurosci 29:5681–5689.

Gossard JP, Brownstone RM, Barajon I, Hultborn H (1994) Transmission in a locomotor-related group Ib pathway from hindlimb extensor muscles in the cat. Exp Brain Res 98:213–228.

Grillner S (1975) Locomotion in vertebrates - central mechanisms and reflex interaction. Physiol Rev 55:247–304.

Grillner S (2006) Biological pattern generation: cellular and computational logic of networks in motion. Neuron 52:751–766.

Grillner S, Kozlov A (2021) The CPGs for limbed locomotion—facts and fiction. Int J Mol Sci 22:5882.

Grillner S, Zangger P (1979) On the central generation of locomotion in the low spinal cat. Exp Brain Res 34:241–261.

Harnie J, Audet J, Klishko AN, Doelman A, Prilutsky BI, Frigon A (2021) The spinal control of backward locomotion. J Neurosci 41:630–647.

Hsu LJ, Zelenin PV, Lyalka VF, Vemula MG, Orlovsky GN, Deliagina TG (2017) Neural mechanisms of single corrective steps evoked in the standing rabbit. Neuroscience 347:85–102.

Huang B, Xiong C, Chen W, Liang J, Sun B-Y, Gong X (2021) Common kinematic synergies of various human locomotor behaviours. R Soc Open Sci 8:210161.

Iwahara T, Atsuta Y, Garcia-Rill E, Skinner RD (1992) Spinal cord stimulation-induced locomotion in the adult cat. Brain Res Bull 28:99–105.

Jansen K, De Groote F, Massaad F, Meyns P, Duysens J, Jonkers I (2012) Similar muscles contribute to horizontal and vertical acceleration of center of mass in forward and backward walking: implications for neural control. J Neurophysiol 107:3385–3396.

Karayannidou A, Zelenin PV, Orlovsky GN, Sirota MG, Beloozerova IN, Deliagina TG (2009) Maintenance of lateral stability during standing and walking in the cat. J Neurophysiol 101:8–19.

Kiehn O (2016) Decoding the organization of spinal circuits that control locomotion. Nat Rev Neurosci 17:224–238.

Krouchev N, Kalaska JF, Drew T (2006) Sequential activation of muscle synergies during locomotion in the intact cat as revealed by cluster analysis and direct decomposition. J Neurophysiol 96:1991–2010.

Lyakhovetskii V, Merkulyeva N, Gorskii O, Musienko P (2021) Simultaneous bidirectional hindlimb locomotion in decerebrate cats. Sci Rep 11:3252.

McCrea DA (1998) Neuronal basis of afferent-evoked enhancement of locomotor activity. Ann N|Y Acad Sci 860:216–225.

McCrea DA, Rybak IA (2008) Organization of mammalian locomotor rhythm and pattern generator. Brain Res Rev 57:134–146.

McLean DL, Fan J, Higashijima S, Hale ME, Fetcho JR (2007) A topographic map of recruitment in spinal cord. Nature 446:71–75.

McLean DL, Masino MA, Koh IY, Lindquist WB, Fetcho JR (2008) Continuous shifts in the active set of spinal interneurons during changes in locomotor speed. Nat Neurosci 11:1419–1429.

Merkulyeva N, Veshchitskii A, Gorsky O, Pavlova N, Zelenin PV, Gerasimenko Y, Deliagina TG, Musienko P (2018) Distribution of spinal neuronal networks controlling forward and backward locomotion. J Neurosci 38:4695–4707.

Murphy PR, Stein RB, Taylor J (1984) Phasic and tonic modulation of impulse rates in gamma-motoneurons during locomotion in premammillary cats. J Neurophysiol 52:228–243.

Musienko PE, Bogacheva IN, Gerasimenko YP (2007) Significance of peripheral feedback in the generation of stepping movements during epidural stimulation of the spinal cord. Neurosci Behav Physiol 37:181–190.

Musienko PE, Zelenin PV, Lyalka VF, Gerasimenko YP, Orlovsky GN, Deliagina TG (2012) Spinal and supraspinal control of the direction of stepping during locomotion. J Neurosci 32:17442–17453.

Musienko PE, Deliagina TG, Gerasimenko YP, Orlovsky GN, Zelenin PV (2014) Limb and trunk mechanisms for balance control during locomotion in quadrupeds. J Neurosci 34:5704–5716.

Musienko PE, Lyalka VF, Gorskii OV, Merkulyeva N, Gerasimenko YP, Deliagina TG, Zelenin PV (2020) Comparison of operation of spinal locomotor networks activated by supraspinal commands and by epidural stimulation of the spinal cord in cats. J Physiol 598:3459–3483.

Orlovsky GN, Deliagina TG, Grillner S (1999) Neuronal control of locomotion. From mollusc to man. Oxford, UK: Oxford UP.

Pratt CA, Buford JA, Smith JL (1996) Adaptive control for backward quadrupedal walking V. Mutable activation of bifunctional thigh muscles. J Neurophysiol 75:832–842.

Quevedo J, Fedirchuk B, Gosgnach S, McCrea D (1998) Group I disynaptic excitation in flexor and bifunctional motoneurons during locomotion. Ann N|Y Acad Sci 860:499–501.

Rancic V, Gosgnach S (2021) Recent insights into the rhythmogenic core of the locomotor CPG. Int J Mol Sci 22:1394.

Rancic V, Ballanyi K, Gosgnach S (2020) Mapping the dynamic recruitment of spinal neurons during fictive locomotion. J Neurosci 40:9692–9700.

Rossignol S (1996) Neural control of stereotypic limb movements. In: Handbook of physiology. (Rowell LB, Sheperd JT, eds), pp 173–216. New York: Oxford UP.

Rossignol S, Dubuc R, Gossard J-P (2006) Dynamic sensorimotor interactions in locomotion. Physiol Rev 86:89–154.

Rybak IA, Dougherty KJ, Shevtsova NA (2015) Organization of the mammalian locomotor CPG: review of computational model and circuit architectures based on genetically identified spinal interneurons. eNeuro 2: ENEURO.0069-15.2015.

Shah PK, Gerasimenko Y, Shyu A, Lavrov I, Zhong H, Roy RR, Edgerton VR (2012) Variability in step training enhances locomotor recovery after a spinal cord injury. Eur J Neurosci 36:2054–2062.

Shefchyk S, McCrea DA, Kriellaars D, Fortier P, Jordan L (1990) Activity of interneurons within the L4 spinal segment of the cat during brainstem-evoked fictive locomotion. Exp Brain Res 80:290–295.

Stein PSG, Mortin LI, Robertson GA (1986) The forms of a task and their blends. In: Neurobiology of vertebrate locomotion, pp 201–216.. London: Macmillan.

Talpalar AE, Bouvier J, Borgius L, Fortin G, Pierani A, Kiehn O (2013) Dual-mode operation of neuronal networks involved in left–right alternation. Nature 500:85–88.

Thorndike RL (1953) Who belongs in the family? Psychometrika 18:267–276.

Thorstensson A (1986) How is the normal locomotor program modified to produce backward walking. Exp Brain Res 61:664–668.

Vanderhorst VG, Holstege G (1997) Organization of lumbosacral motoneuronal cell groups innervating hindlimb, pelvic floor, and axial muscles in the cat. J Comp Neurol 382:46–76.

Vemula MG, Deliagina TG, Zelenin PV (2019) Kinematics of forward and backward locomotion performed in different environmental conditions. J Neurophysiol 122:2142–2155.

Vilensky JA, Cook JA (2000) Do quadrupeds require a change in trunk posture to walk backward? J Biomech 33:911–916.

Ward JH (1963) Hierarchical grouping to optimize an objective function. J Am Stat Assoc 58:236–244.

Yokoyama H, Kato T, Kaneko N, Kobayashi H, Hoshino M, Kokubun T, Nakazawa K (2021) Basic locomotor muscle synergies used in land walking are finely tuned during underwater walking. Sci Rep 11:18480.

Zelenin PV, Deliagina TG, Orlovsky GN, Karayannidou A, Stout EE, Sirota MG, Beloozerova IN (2011) Activity of motor cortex neurons during backward locomotion. J Neurophysiol 105:2698–2714.

Zelenin PV, Vemula MG, Lyalka VF, Kiehn O, Talpalar AE, Deliagina TG (2021) Differential contribution of V0 interneurons to execution of rhythmic and nonrhythmic motor behaviors. J Neurosci 41:3432–3445.

Zelik KE, La Scaleia V, Ivanenko YP, Lacquaniti F (2014) Can modular strategies simplify neural control of multidirectional human locomotion? J Neurophysiol 111:1686–1702.